A Novel Battery Supported Energy Management System for the Effective Handling of Feeble Power in Hybrid Microgrid Environment

SIVASANKAR GANGATHARAN[1]**, (Member, IEEE), MAGESWARAN RENGASAMY**[1]**, RAJVIKRAM MADURAI ELAVARASAN**[2]**, NAROTTAM DAS**[3,4]**, (Senior Member, IEEE), EKLAS HOSSAIN**[5]**, (Senior Member, IEEE), AND VARATHARAJAN MEENAKSHI SUNDARAM**[1]

[1]Department of Electrical and Electronics Engineering, Thiagarajar College of Engineering, Madurai 625015, India
[2]Clean and Resilient Energy Systems Laboratory, Texas A&M University, Galveston, TX 77553, USA
[3]School of Engineering and Technology, Central Queensland University, Melbourne, VIC 3000, Australia
[4]Center for Intelligent Systems, Central Queensland University, Brisbane, QLD 4000, Australia
[5]Department of Electrical Engineering and Renewable Energy, Oregon Renewable Energy Center (OREC), Oregon Institute of Technology, Klamath Falls, OR 97601, USA

Corresponding authors: Rajvikram Madurai Elavarasan (rajvikram787@gmail.com) and Eklas Hossain (eklas.hossain@oit.edu)

ABSTRACT One of the crucial challenges in the present power distribution system is the conversion loss phenomenon. Modern microgrid integrates various converters for varieties of applications, such as distributed power generation interconnection, energy storage management system, grid integration, demand management, etc. The increased usages of power converters further worsen the existing situation. Any initiatives taken towards energy conservation go in vain due to the excessive conversion loss phenomenon in the present distribution schemes. In this regard, a novel microgrid energy management scheme is proposed and developed to reduce the conversion losses in the residential distribution system. It uses a new control algorithm that finds the strength of power available in the DC side before being transferred. The conversion process is invoked only if the power is adequate, and if found feeble, then the conversion process is withdrawn and stored in an auxiliary battery. Conversion of feeble power would result in high loss across the converters and transformers. In this scheme, the AC loads are supplied by the utility grid, and the DC loads are fed by a solar PV and an auxiliary battery bank. The power conversion is done only during unavoidable circumstances. A prototype hardware setup has been developed, and the objective of the proposed research task has been validated. Further, the proposed scheme would gain importance in reducing the cost of the electricity for a time-of-use tariff system by optimization. A genetic algorithm is proposed to optimize the energy management of the microgrid system.

INDEX TERMS Battery based energy management system, solar PV, hybrid microgrid, conversion loss reduction, energy saving.

I. INTRODUCTION

One of the important challenges in the present power distribution system is the conversion loss phenomenon. Nowadays, the usage of DC appliances has been increasing significantly. In this scenario, there is a remarkable increase in the usage of DC operated equipment in daily lives [1]. Usually, the DC loads are plugged into the AC terminals due to the unavailability of separate DC supply systems at

The associate editor coordinating the review of this manuscript and approving it for publication was Huiqing Wen.

the consumer premises. The AC power is customized using converters for various DC load requirements and it results in multiple conversions. The conversion losses and harmonics produced by the converters are significantly increasing day by day and polluting the power system network. These conversion processes render an average power loss of 10-30% [2]. Further, the photovoltaic (PV) systems generate DC power. To respond to the growing use of DC systems, and to accommodate the low power distributed generation resources, the concept of microgrid has been evolved. The microgrid offers several advantageous features; it includes

remote electrification, optimal usage of the renewable energy system [3]. It suits well with developing smart grid activities and enhances the Battery Energy Storage System (BESS) [4]. But, when a BESS is connected to the conventional AC terminals, enormous conversion losses are encountered due to various conversion processes. So, the efficiency of BESS has deteriorated. But in a microgrid environment, the BESS is operated within the DC bus for most of the time. Hence, the losses encountered in the charge processes drastically reduce, therefore, the performance of the BESS is significantly improved in a microgrid topology. However, due to the intermittent characteristics, microgrids built with solar PV constitute several technical challenges [5]–[7]. Even after the introduction of hybrid AC/DC microgrid, the power conversion process is invoked frequently during the deficit of power in the microgrid environment. In optimization strategy, the energy cost is minimized by deploying energy storage devices for peak demand management, and they are charged during off-peak hours. Many hours in a day, the batteries are charged from the utility grid supply. This scenario resurfaces the conversion process and results in excessive conversion loss.

In the existing literature, energy management systems and intelligent techniques have been used to address several phenomena such as the optimal deployment of sources, scheduling the loads based on priority, load shedding, peak demand management, and energy storage management [8]–[10]. There are various control algorithms and flowcharts used in literature to operate the microgrid. In the literature [11], [12], the renewable energy system's power availability is checked with the load requirement and the demand is met. Further, the batteries are deployed concerning its charge status. The interlinking DC voltage variation is used as a reference to manage energy systems [13]. In [14], the battery bank voltage level is used to operate the battery backup. In the optimization-based control technique, cost minimization has been taken as an objective function to handle the microgrid energy management [15], [16]. The battery management strategies focus is towards peak demand management for economical energy cost, optimizing cost by operating at minimal tariff. Similarly, batteries deployed in standalone microgrid systems are operated only during power intermittency and during the unavailability of renewable power.

The surveyed literature so far indicated that various conditions and thresholds are used to control the conversion processes. However, two important scenarios have not been addressed during the AC/DC power conversion process. First, the export of solar power through the interlinking converter will be effective only if it is of sufficient quantity. The conversion will be invoked when the solar PV power availability is in low quantity and it will result in more losses across the converter than the requirement for which it has been intended. Secondly, in a situation, where the solar power is unavailable and the DC side load requirement is less, importing power from the utility will result in relatively more power losses across the converter than the requirement.

The aforementioned power conversion processes occur frequently in a microgrid environment. The major reason is that the converters and transformers exhibit poor performance when operated at under loaded conditions [17]. The conversion will process when the power availability is less than 20% of the rated value and it will exhibit poor performance [18]. This scenario has been illustrated elaborately in Section III using an experimental inference furnished in Fig. 4 and Equation (8) has been derived in this regard. This lower value of power is mentioned as feeble power in this work. To emphasize the uniqueness of the proposed work, a comparative study has been presented in Table-1. The best solution for the aforementioned scenario is to effectively manage BESS to handle the feeble power of the renewable-based microgrid system and to maximize energy efficiency.

TABLE 1. Comparison of the proposed strategy with the existing literature.

Literature	Tariff Cost reduction	Peak Demand	Intermittency Support	Stand-Alone Mode support	Voltage Regulation	Routine utilization	Feeble Energy conservation
[19]	X	X	✓	✓	✓	X	X
[20]	✓	✓	✓	X	X	X	X
[21]	✓	✓	✓	✓	✓	X	X
[22]	✓	✓	✓	✓	X	X	X
[23]	X	X	✓	✓	✓	X	X
[24]	X	X	✓	✓	✓	✓	X
[25]	✓	X	✓	✓	X	X	X
[26]	X	X	✓	✓	✓	X	X
[27]	X	X	✓	✓	✓	X	X
Proposed Scheme	✓	X	✓	✓	✓	✓	✓

It has been inferred that 14-25% of energy savings can be attained by storing excess power using storage devices such as a battery [28], [29]. It is reported that Germany has announced the incentive of €50 m for solar-based BESS and the subsidies cover 30% cost of their battery system [30]. Similarly, Italy has provided an incentive for residential PV based storage [31]. Further incorporating the best practices for improving battery life is essential for emphasizing sustainability and reliability [32], [33].

In this regard, the proposed research study is to design a novel battery-based energy management system to efficiently manage the solar PV hybrid microgrid for the residential distribution system. In this work, the residential distribution within the consumer premises has to be restructured with a smart distribution system comprising a hybrid AC/DC microgrid to exhibit better compatibility with renewable energy sources, energy storage, and various loads.

The newer energy management strategy aims to:
- Effectively handle feeble PV power prevailing in the DC side of the microgrid using an auxiliary battery setup to conserve energy.
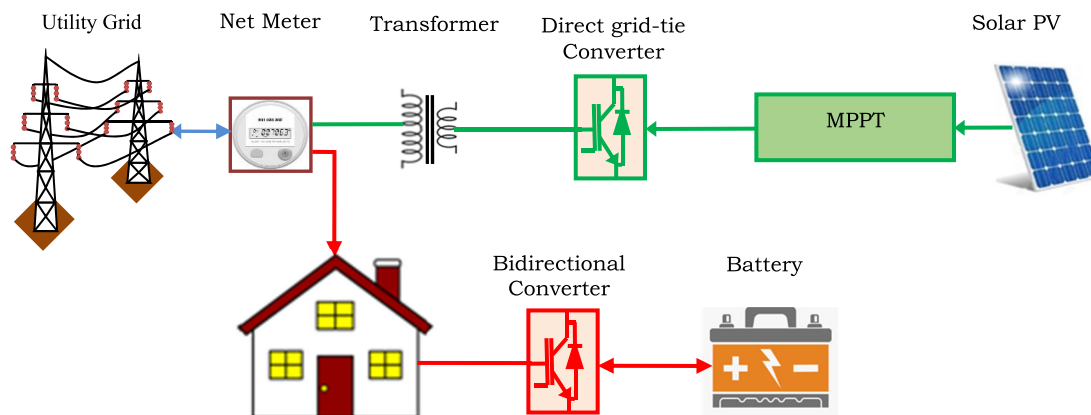
FIGURE 1. Direct utility-grid tied PV system where the generated PV power is completely fed into the utility grid and a separate supply line is wired for the residential loads to solve the intermittency problem caused in a stand-alone scheme.

- Efficiently manage solar PV, battery storage, and loads to enhance energy saving and reduce conversion losses.
- Realize cost-effective power distribution using genetic algorithm based optimization.

Existing solar PV based residential electrification schemes have been discussed in Section II. The factors limiting the performance of microgrid and the BESS have been discussed in Section III. Section IV describes the proposed hybrid AC/DC microgrid topology. The description of configurations of solar panel, BESS, and converters used in the microgrid are depicted in subsection IV (A), IV (B), and IV(C) respectively. The newly developed Battery Energy Storage based management strategy and the centralized microgrid controller operations are explained in Section V. Conversion loss reduction strategy has been illustrated in Section VI. Results and discussions are furnished in Section VII. This section includes a discussion about the hardware prototype design and subsection VII (A) illustrates the beneficial characteristics of the proposed microgrid scheme in comparison with a direct grid-tied scheme and conventional microgrid scheme.

II. EXISTING SOLAR PV BASED RESIDENTIAL ELECTRIFICATION SCHEMES

Generally, solar PV deployment in the residential premises is configured as direct grid-tied or standalone PV schemes. Since solar PV power is intermittent, PV based stand-alone supply system is not preferred and a direct grid-tie scheme is utilized commonly as shown in Fig.1. In the direct grid-tied scheme the generated PV power is completely fed into the utility grid and a separate supply line is wired for the residential loads. This scheme uses a net meter to account for the export and import of power. The advantage of this scheme is that the maximum power is extracted every time from the PV panel using the Maximum Power Point Tracking (MPPT) system. However, this scheme has a limitation that every time the generated DC power is inverted to AC. Hence, the inverter loss is inevitable. The efficiency of the inverter is better

when handling the rated quantity of power, and exhibits poor performance during under loaded conditions. Most of the time, the inverters are operated at the under-loaded condition and the losses were always predominant.

The microgrid technology has got its significance to address the aforementioned issues. However, even after the evolvement of microgrid technology, rooftop solar PV technology couldn't establish its attention. Globally, people do not have a positive insight about adopting the rooftop solar PV in their residential premises due to its high capital cost and prolonged payback period.

III. FACTORS LIMITING THE PERFORMANCE OF MICROGRID AND BESS

Globally, the attention towards solar-based renewable energy is increasing rapidly, there are many renewable role player countries like India and China that are consistently showing their improvement in terms of implementing new renewable energy technologies and also there are a lot of steps taken by them to overcome the barriers by implementing effective governmental policies in the structure of existing power distribution system [34]–[36]. The energy management system plays a major role to manage efficiently all the variability and intermittencies in the energy sources, perpetual power supply, and different types of storage devices to provide reliable and endurable power [7], [37]. Battery Energy Storage (BES) has a wide range of applications in microgrid energy management. It is inferred that the ESS enhances power quality [38], and supports stand-alone microgrid operation, active distribution systems, and Plug-in Electric Vehicles (PEVs) technologies. The PEV improves the voltage profile, frequency regulation, dynamic and transient stability [39], [40]. Besides, it also minimizes energy costs [41]. It enhances the stability and assists the supportive services, such as outage protection, peak shaving, and grid power control. It is also essential to effectively operate the converters connected with the network [42]. But the efficiencies of these converters vary over a wide range. Therefore, it is not always clear for a user how
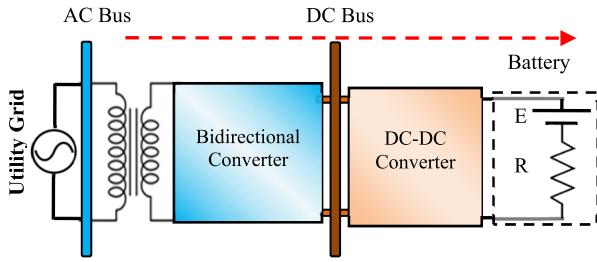
FIGURE 2. Battery charging in a microgrid environment fed by the utility.

much energy is lost in the conversion process when it is executed. The efficiency of the BESS is claimed as 90-95% [43], but in a real-time scenario, the overall efficiency of the BESS deteriorates [44]. Similarly, the hybrid DC-DC converter efficiency is claimed as 95% [45], while considering the internal loss of battery, it exhibits only 90% [46]. To understand the actual loss scenario, the charging and discharging processes of the BESS are elaborated as shown in Fig.2. This process applies to BES management in the microgrid environment as well. The power loss occurs at various stages and it is different during the charging and discharging process. The following expression represents the loss phenomenon during charging the battery.

$$P_{chg,loss} = P_{int,loss} + P_{dc.conv,loss} + P_{rect,Loss} + P_{trs,loss}. \tag{1}$$

where $P_{int,loss}$ is the battery internal loss, $P_{dcconv,loss}$ is the loss in the DC converter of the charging circuit, $P_{rect,Loss}$ is the loss across the rectifier and $P_{rect,Loss}$ is the transformer loss. During the discharge of the battery, the following losses are encountered.

$$P_{dis,loss} = P_{int,loss} + P_{dc.conv,loss} + P_{inv,Loss} + P_{trs,loss}. \tag{2}$$

where $P_{inv,Loss}$ is the loss across the inverter during power conversion.

The losses in an inverter are calculated by the following equations:

$$\begin{aligned} P_{inv,loss} &= 4 * P_{SW,IGBT} \\ &= 4 * \frac{(E_{on} + E_{off}) \times I_{pk} \times f_{SW} \times V_{dc}}{\pi \times I_{nom} \times V_{nom}}. \end{aligned} \tag{3}$$

where E_{on} and E_{off} are energy loss during turning ON and OFF the switch respectively, I_{pk} is the peak current, f_{SW} is the switching frequency, and I_{nom}, V_{nom}, are nominal current and voltage respectively.

Similarly, a diode loss comprises of conduction and reverse recovery losses.

$$P_{diode,loss} = P_{d.cond,loss} + P_{d.rev,loss}. \tag{4}$$

where $P_{dcond,loss}$ is diode conduction loss and $P_{drev,loss}$ is diode reverse recovery loss.

The conduction and switching losses of the switches used in the converters vary over a wide range concerning the load.

The detailed information about the converter loss parameters and their efficiency details can be inferred from the Ref. [47]. The BESS undergoes various conversions and renders enormous losses in its charge processes. This scenario reduces efficiency as well as weakens its life cycle. The BESS fed by the solar PV system is shown in Fig.3, where the battery system is maintained within the DC bus, the loss occurrence is less due to reduced conversion stages. The expression of loss possibility can be found from the equation as given in equation (5):

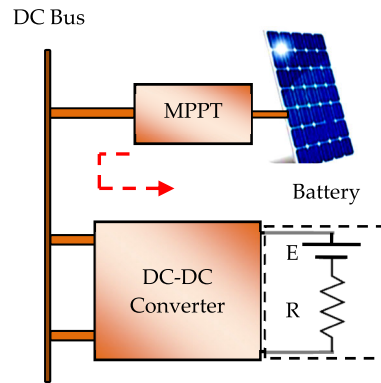$$P_{batt,loss} = P_{int,loss} + P_{dcconv,loss}. \tag{5}$$

FIGURE 3. Battery charging in a DC microgrid environment fed by solar PV power.

The batteries are an essential part of residential premises. In a conventional microgrid system, the battery charging process is similar to that of a conventional system comprising a transformer, rectifier, and DC-DC converter. A considerable amount of power is dropped in this conversion process, and the experimentation has been carried out to identify the performance of the battery in the laboratory. The experimental observation and the respective efficiency curves are shown in Fig.4.

The efficiency of the microgrid system depends on several loss criteria. Standalone inverter efficiency reaches about 85-90% only when it is operated more than two-third of its rated capacity and it reaches a maximum when it is fully loaded.

Its efficiency sharply decreases, when it is underutilized and can reach less than 50% when it is lightly loaded [17]. Hence, any conversion process will lead to a significant quantity of loss and related consequences as well. Usually, the people widely prefer inverters in the local market for its low price, but their performance is questionable. An inverter used in the consumer premises is tested for its efficiency. The experimentally inferred efficiency graph is shown in Fig.5. The efficiency of the solar energy conversion process is highly affected by the performance of these local inverters.

It has been inferred that the inverter efficiency reaches above 85%, only when it is operated with 80% of the rated value. Poor efficiency of 52.3% has been recorded during the lightly loaded condition. The aforementioned scenario has
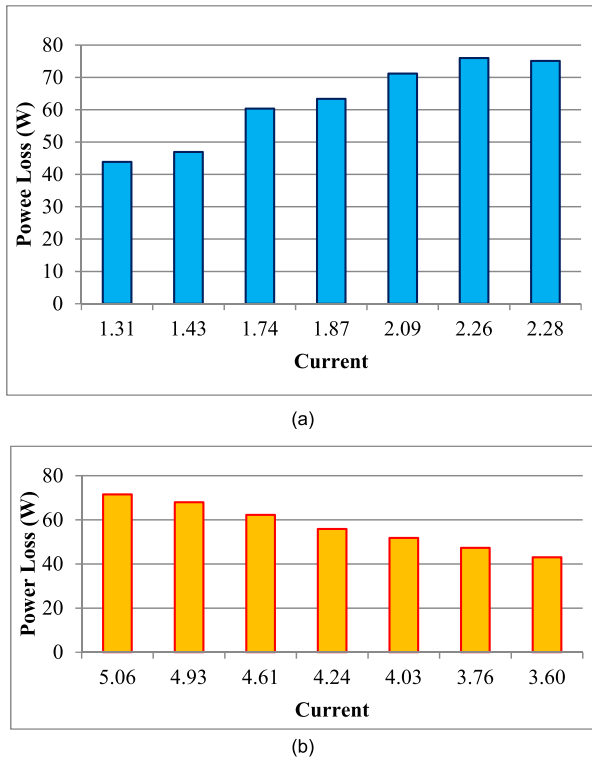
(a)

(b)

FIGURE 4. (a) Power loss during battery charging and (b) Power loss during battery discharge.
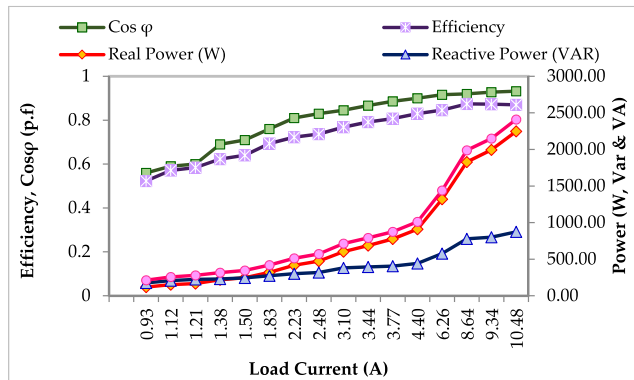

FIGURE 5. Performance characteristics of the inverter used in customer premises.

been reported in [18] as well. Most of the time, the inverters are lightly loaded and hence an excessive amount of power is wasted in the inversion process. An expression for identifying the of the interlinking converter is deduced from the experimental results using a polynomial fitting function and it is depicted as shown below,

$$f(x) = 0.00438x^2 - 0.14984x^2 + 1.97526x^2 - 12.74577x^2 \\ + 42.33597x + 22.98449 \quad (6)$$

where x is a variable representing the current parameter.

This expression can be used to deduce the performance of the converter for calculating the power loss for any new value

of the power conversion process. The efficiency obtained using the evolved expression has exactly correlated with the experimental value; it is shown in Fig.6. The conversion losses have been obtained and shown in Fig.7.
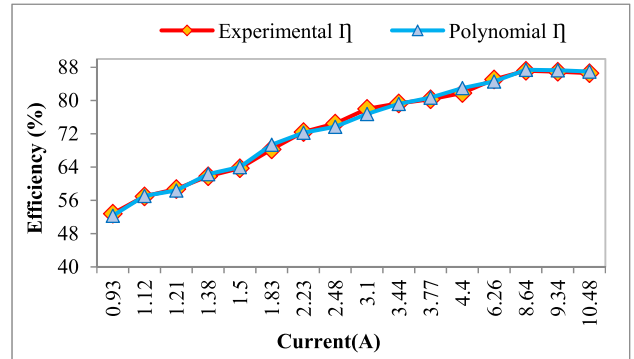

FIGURE 6. Comparison of efficiency values obtained using experimentation and polynomial fitting function.
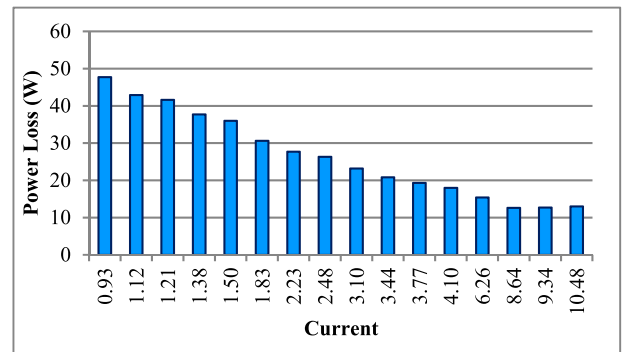

FIGURE 7. Bidirectional converter loss profile.

IV. PROPOSED MICROGRID SYSTEM DESCRIPTION

This research aims to construct a renewable resource-based hybrid AC/DC microgrid and to implement the Advanced Distribution Management system. Introducing the DC distribution through the DC microgrid technology is praised due to their high efficiency, consistency, reliability, and load sharing performance when interconnected to the DC renewable and storage sources. In this work, the power demand of microgrid consumers is met by a small scale autonomous solar PV system which also operates efficiently under both grid-connected and standalone mode.

The proposed AC-DC microgrid schematic representation is shown in Fig.8. The integration of renewable energy resources like the PV, battery, etc. with a low voltage system will be a feasible solution to reduce multiple energy conversion losses in the proposed system.

A. CONFIGURATION OF PV PANEL
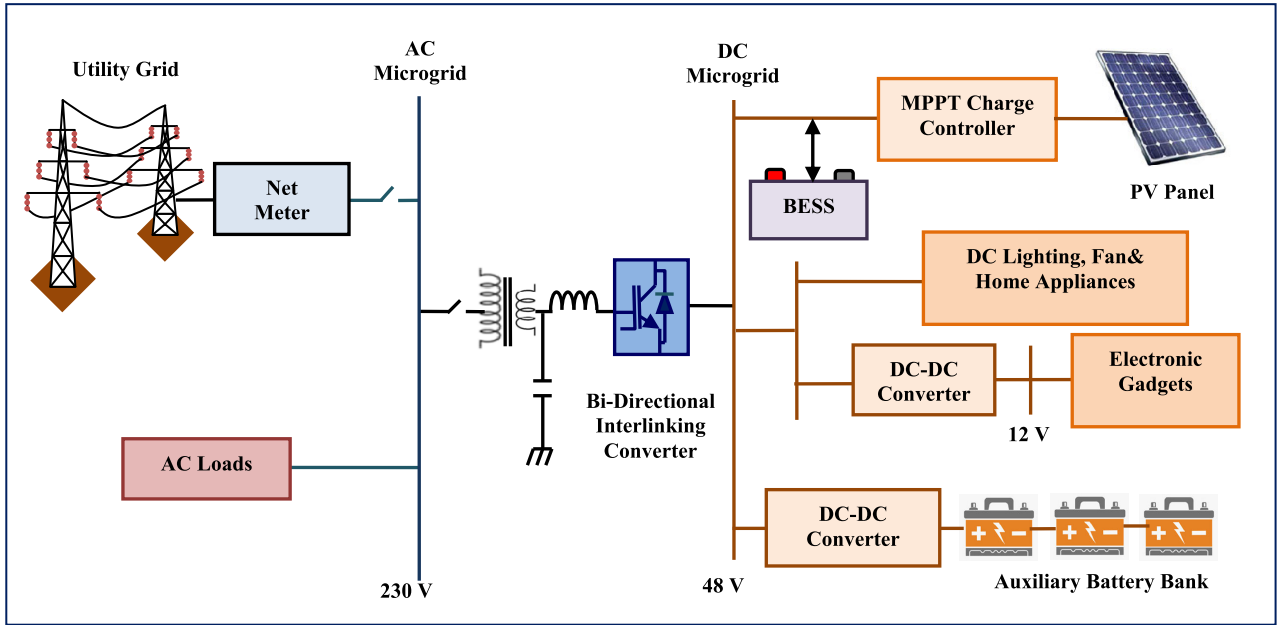The renewable source considered for the proposed system is a solar PV with one diode model because it is simpler

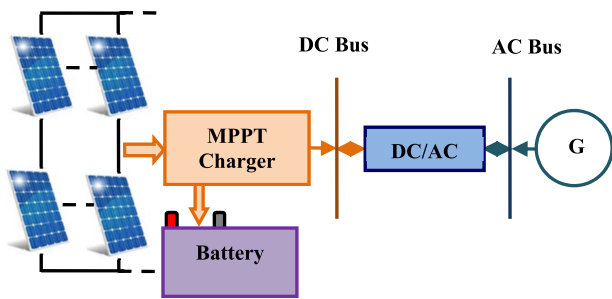**FIGURE 8.** Proposed solar PV based hybrid AC/DC microgrid configuration.

FIGURE 9. PV module configuration setup which contains five parallel combinations of two panels configured in series.
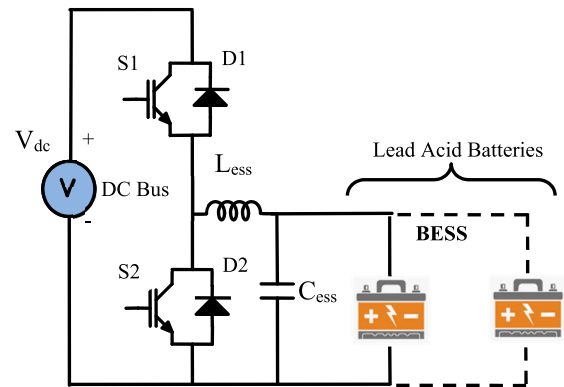

FIGURE 10. Bidirectional DC-DC converter configuration for Battery Energy Management.

and provides an accord between simplicity and accuracy. In the proposed work, ten PV panels (Model No: DSP 100) of 100 W have been used. To have a terminal voltage of 48 V, five parallel combinations of two panels are configured in series as shown in Fig.9.

B. BESS CONVERTER CONFIGURATION

In a DC microgrid system, a suitable voltage level is chosen to avoid few conversion stages and to supply energy resources reliably and efficiently. The DC network has a solar panel feeder at the voltage level of 48 V. The ESSs have been connected to the DC bus through a bidirectional DC converter as shown in Fig. 10. Generally, the DC-DC converter systems are used as interfacing between the DC bus and energy storage device, so reduce fluctuations in the DC voltage.

The efficiency, reliability, and dynamic performance of the system hinges on the operation of the bidirectional converter under various modes of operations so that the individual parts of the system can operate suitably.

Mode 1: During battery charging, the switch S_1 and diode D_2 operate and the converter acts as buck mode.

Mode 2: When the battery power is required for feeding the load during power outages the switch S_2 and diode D_1 conduct and the converter works in boost mode to meet the DC bus demand.

Mode 3: If the battery power is not in use, it is put in float mode (trickle charging mode) to maintain the voltage and SoC at an appropriate level.

The State of Charge (SoC) of the battery has been obtained using the Open Circuit Voltage (OCV) method as in Ref. [48]. The SoC of a battery linearly varies concerning the OCV variation. The relationship between the SoC of the lead-acid battery and its OCV is given by the following equation

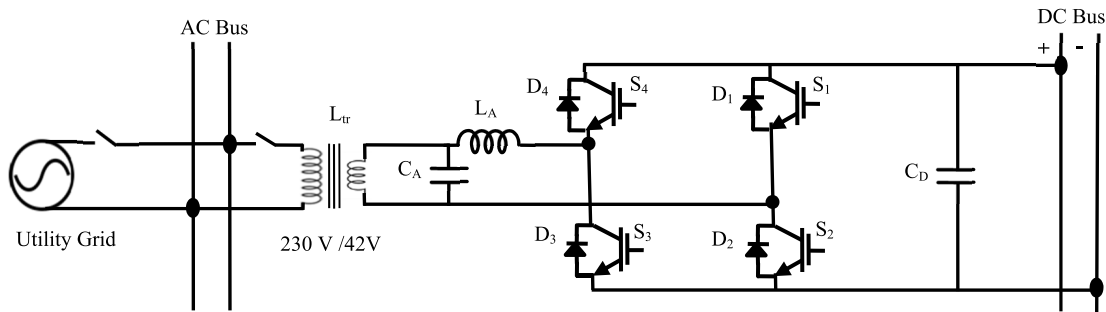$$V_{OC}(t) = a_n X \, SoC(t) + a_0, \tag{7}$$

FIGURE 11. Microgrid bidirectional interlinking converter configuration, where AC and DC buses are attached by a bidirectional interlinking converter.

where a_0 is the battery terminal voltage when SoC = 0% and a_n is obtained by knowing the open-circuit voltage of the battery when SoC is 100%.

C. MICROGRID CONVERTER CONFIGURATION

The schematic diagram of the AC/DC microgrid converter configuration is shown in Fig.11. It consists of AC and DC buses attached by a bidirectional interlinking converter, which is responsible for power transfer between two buses [49]. The IGBT switches are operated using (need to define) SPWM based gate switching at a frequency of 10 kHz. The gate pulses are ignited only when the inversion is intended. Two solid-state switches S_U and S_C are used to invoke power flow, S_U is a utility connect switch and S_C is a converter connect switch. The DC bus is maintained at 48 V. There is several voltage levels, such as 400 V, 326 V, 220 V, 120 V, and 48 V are in practice. However, 48 V is widely preferred for low voltage DC systems [50], and it is referred to as an optimal voltage for low power residential requirements [51].

The solar MPPT charge controller and the BESS converters are regulated to maintain a stiff DC bus voltage. In a situation, where the generated solar power is abundant, it will be exported to the grid for grid storage [52]. In autonomous or independent mode, the battery plays a vital role in energy balance and voltage stability requirements through charging and discharging controls [53], [54].

V. MICROGRID CONTROLLER

The newly designed microgrid consists of an automatic centralized controller that provides coordinated control and it monitors the overall functions of the microgrid. The microcontroller ATMEGA328 has been used to execute the entire control operation of the EMS. The controller block diagram is shown in Fig.12. The main purpose of this centralized controller is to check the capability of meeting the imprudent load demand and to schedule its operation accordingly for proper/ smooth operation. The solar MPP boost converter gate signal is modulated using operated using PWM generated using the P & O algorithm.

The grid integration control angle is inferred using the following pair of equations;

$$tan\varphi = \frac{\omega_1 L_l I_{AC}}{V_{ac}}. \tag{8}$$

$$V_{ac} = \sqrt{V_g^2 + (\omega_1 L_l I_{AC})^2}. \tag{9}$$

$$L_l = L_A + L_{tr}. \tag{10}$$

$$L_{tr} = E_{lp} + E_{ls}. \tag{11}$$

The PI controllers establish closed-loop control of converter operation. The PI parameters are, $k_P = 0.84$ and $K_I = 1.26$ for bidirectional converter control, and $k_P = 0.035$ and $K_I = 0.156$ for MPP boost converter. The PI controller values have been obtained using the Ziegler–Nichols tuning technique. The designed microgrid structure has been operated with an automatic centralized controller.

The controller monitors the overall performance/ function of the microgrid. In the proposed scheme, a threshold value of 20% of the system rating is fixed for invoking the converter operation since the losses in the conversion processes are accounted to be varying between 13-18% (Inferred as shown in section 1.3). If power conversion is processed below this threshold, it will lead to ineffective power output. The proposed power control flow chart is shown in Fig.13.Various operations of the microgrid control are accomplished using the algorithm that stated in the flow chart is as follows:

- Initially, all the DC side of the microgrid power variables are measured, i.e., power at the PV array terminals, battery power, and DC load requirement. The PV panel installation has been performed for 1 kW, which is capable of satisfying mainly the DC side loads and partly the AC loads
- The net PV power (P_N) available after meeting the power required for battery charging (P_{BC}) with MPPT and DC side load requirement (P_{DCL}) is calculated using the equation (14) as follows:

$$P_N = P_{pv} - (P_{BC} + P_{DCL}). \tag{12}$$

Now, the net power P_N is checked, whether it is positive. If the condition is true, the P_N has to be checked whether it is higher than 20% of the rated value. The interlinking
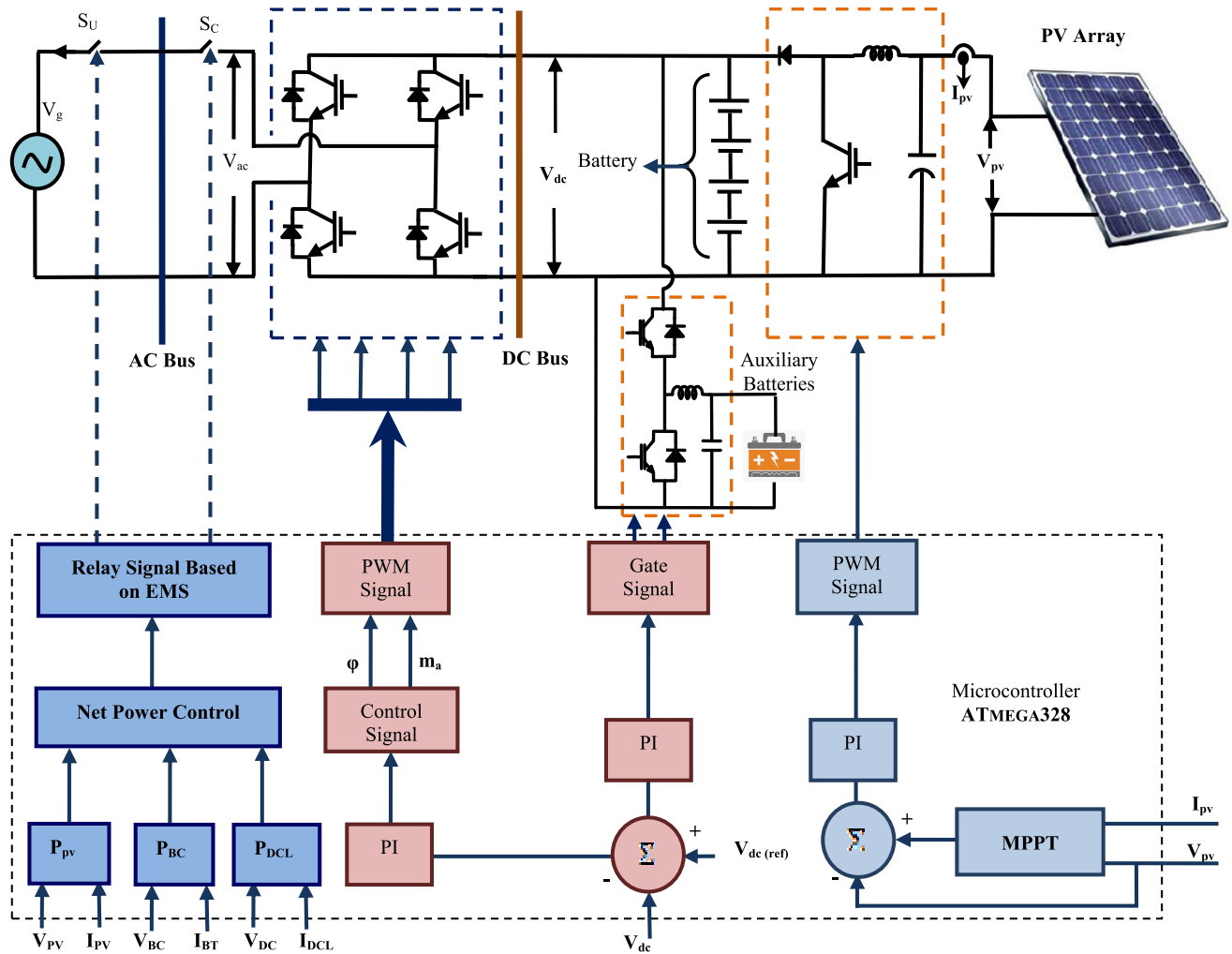
FIGURE 12. Schematic diagram of the proposed microgrid centralized controller.

bidirectional converter exhibits enormous losses when operated below this value, the experimental results of the converter loss profile was shown in Figure. 7 in section 1.3. Hence, any power transferred less than 20% (feeble power) will not seek any benefit. Consequently, the net power in the DC side is checked, if it is available more than 20%. If the condition is satisfied, then switch S_C is turned ON and the power is transferred using inverter mode to feed loads connected to the AC bus. If the condition is not true the available power is stored in the auxiliary battery for future usage.

- If the P_N is negative, it is inferred that the DC side power requirement is not met by the power generated by the solar PV. In this scenario, it is checked whether the power requirement is less than 75% of the rating and if it is true, the SoC of the battery is checked. If SoC is more than 50%, the battery power is utilized for meeting the DC side load demand. The SoC of the battery is checked for its minimum threshold. If it is met, then it is placed (or put) in charge mode and the loads are fed in from

the utility. If the P_N is negative and the load requirement is greater than 75% of the rated, the S_C is turned ON, the utility power is rectified and the DC side loads are fed.

- On the other hand, if the SoC of the battery bank power is less than 50%, the availability of solar power is checked for charging. The batteries are charged only when the solar power is available, if not, it is placed (or put) in standby mode to wait until the availability of solar power.

- Finally, the P_N is checked, if it is equal to P_{ACL}, if it is true, then the available power is fed into AC-bus loads. If the condition is not satisfied, then the power may be excess or deficit. On such occasions, the S_U is turned ON to import or export power. Generally, the switches S_C and S_U are in the OFF state.

VI. CONVERSION LOSS REDUCTION STRATEGY

In this section, the newer feeble conversion loss reduction strategy incorporated in the centralized controller has been
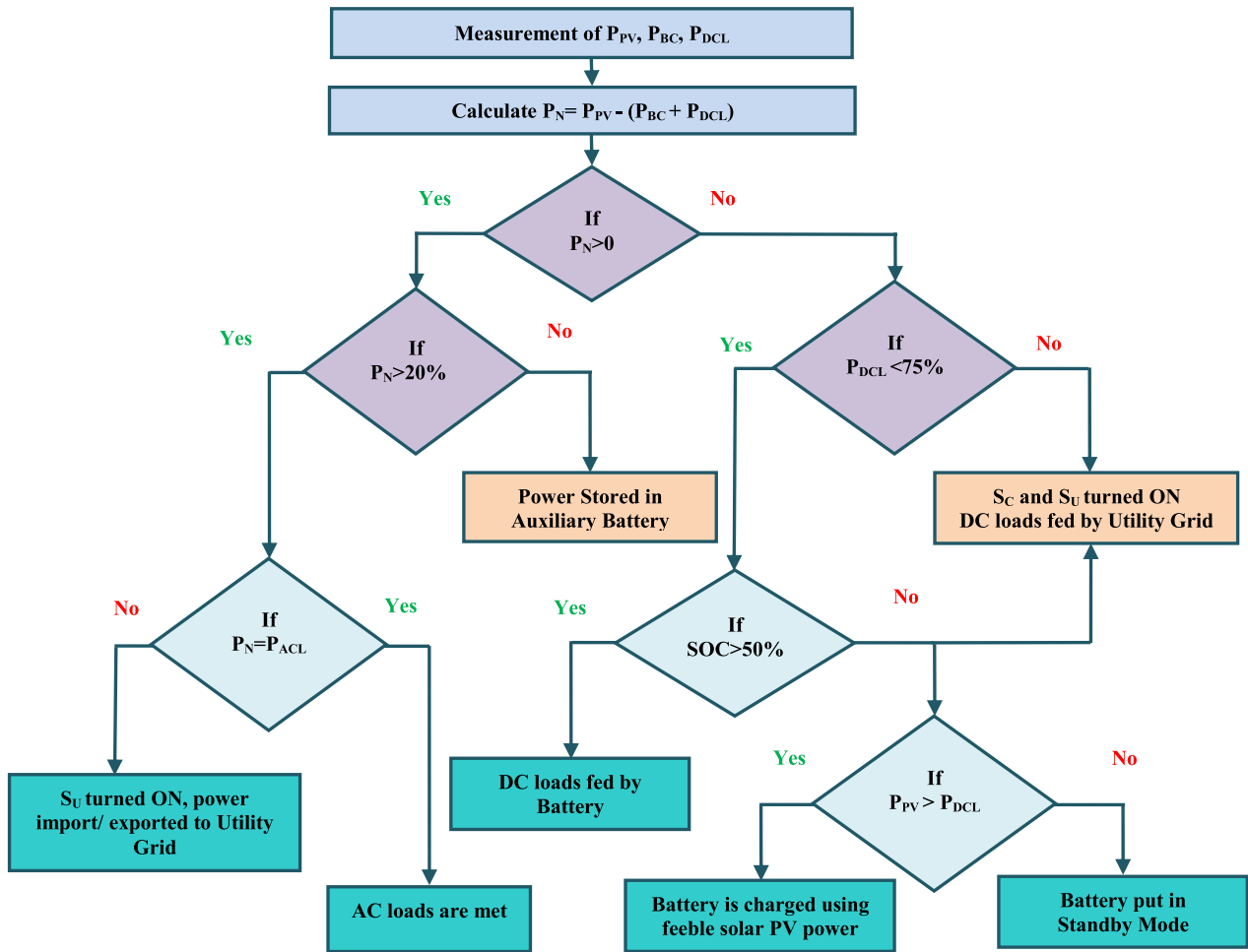
FIGURE 13. Flow chart representation of Automatic Centralized Controller operation.

illustrated. There are several occasions where feeble power prevails in the microgrid system. Three cases have been discussed to illustrate the phenomenon; pictorial representation has been shown in Fig.14.

Case 1: When solar power production is low (7.00 AM to 8.00 AM & 4.00 PM to 5.00 PM), usually the loads would be fed by the utility, and the solar power will be left unutilized. On such occasions, the DC loads connected to the DC bus of the microgrid system are fed from the utility by power conversion. In the proposed scheme the DC loads are fed by the available solar power with the support of an auxiliary battery. The AC loads are fed by the utility. By executing such energy management the conversion process is minimized.

Case 2: During the period 8.00 AM to 9.00 AM & 3.00 PM to 4.PM the solar PV generates a power that is just adequate to supply DC side loads and a feeble amount of power remains after that. The existing literatures have not focused on this scenario. There is no proper strategy found in any of the literatures to

address the feeble solar power which occurs on several occasion in a day. In the conventional schemes, such feeble power is transferred to AC Side through the inverter. But the inverters exhibit poor performance if it is not loaded to its rated value. Hence the feeble power cannot be converted effectively and it is dissipated during the conversion process. To address this phenomenon a control strategy has been developed where the feeble power is stored in an auxiliary battery. This strategy exhibits dual advantage, one is that, the feeble power is conserved and the other is that the battery is charged in a DC environment.

Case 3: During late-night hours (10.00 PM to 5.00 AM), the DC side load requirement is low. Importing power from the utility to feed such low power requirements will result in more amount of loss across the transformer and converter components than the actual requirement. To address this issue, the auxiliary batteries are deputed to feed the DC loads. Further, the battery is checked for its SoC
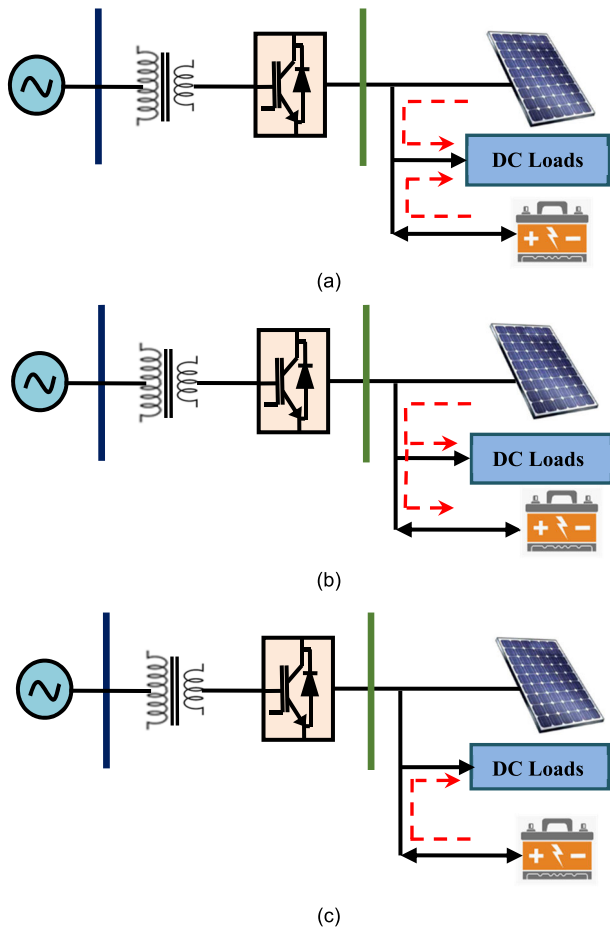
FIGURE 14. The period during which feeble power prevails in the system (a) Case 1 (b) Case 2 (c) Case 3.

FIGURE 15. Experimental setup of the proposed microgrid module.

TABLE 2. Hardware setup ratings for microgrid design.

Equipment	Single Unit	Module	Model
Solar PV	$V_{oc} = 26V$, $I_{SC} = 4.9$ A, $V_{MP} = 22V$, $I_{MP} = 4.1A$	$V_{OC} = 48V$, $I_{SC} = 24.6A$ $V_{MP} = 42V$, $I_{MP} = 4.1A$	DSP100
Battery at solar terminals	100 Ah, 12 V	200Ah, 24V	Amaron
Battery bank	100Ah, 12 V	400Ah, 48 V	Amaron
DC loads	100W	500 W	Set of five resistive loads
AC Load	-	500W, 0.9 PF	Induction motor load
Bidirectional Converter	-	1.2 KVA	Liebert. ESU
Filter	L = 1.2 mH, C= 3.3 μF	-	-
Transformer	230V/42V	-	1 φ, step-down

periodically to avoid deep discharge. During the above mentioned period, feeble power prevails in the DC network of the microgrid. The export or import of power during such an occasion will not be effective. Hence the control strategy and the threshold value have been coined in such a way that the feeble power is handled and stored effectively by the auxiliary battery bank. Hence, power-saving possibilities are improved.

VII. RESULTS AND DISCUSSIONS

A prototype hardware module has been developed in the laboratory for experimentation of the proposed strategy shown in Fig. 15. The module components and specifications are tabulated in Table-2. The total installed capacity of solar PV is 1 kW and the interlinking bidirectional converter is rated as 1kW with a grid-tie option. It is designed with the IEC 62040-3 standard which adheres to grid code requirement and microgrid compliances. The utility source in the laboratory has been considered as the AC source and the experiment has been carried out.
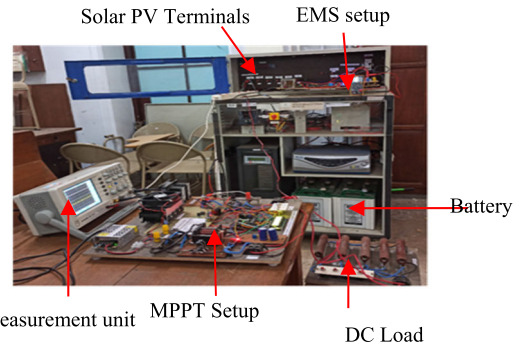
The solar PV is operated at its MPP and stored in a battery rated 200 Ah. This battery has been depicted for acquiring power from solar panels and presented to the DC bus at boost mode. Another set of battery bank with 400 Ah capacity has been linked with the DC bus through the DC-DC converter. This battery bank regulates the DC bus voltage and also meets the DC bus demand. The DC bus distribution is operated with the IEEE P2030.10, a standard for DC Microgrids Electricity Access Applications. The overall microgrid is designed to operate with the IEEE 1366-2012 standards for compliance of Power Distribution Reliability.

The microgrid module is developed and experimented under varying solar irradiation, and the respective load management is inferred. The solar irradiation and temperature values are taken from the NREL website [55] for the research location (Lat, Lon: 9.95, 78.15). The dynamically varying PWM switching signal of the solar PV MPP boost converter and corresponding voltage values are observed using the hardware setup are shown in Fig.16.The voltage and current values of the inverter have been measured using Krykard ALM 35 Energy Analyzer It is shown in Fig.17 (a). From the inverter output voltage, it is inferred that the (better to define) THD is within the prescribed standard, and the voltage THD is shown in Fig.17 (b). The power parameters are
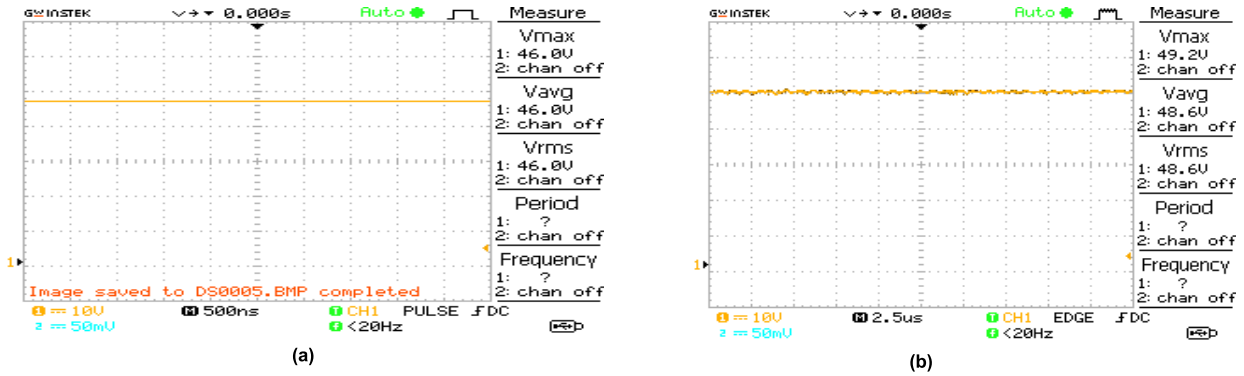
FIGURE 16. (a) Solar panel terminal voltage during medium irradiation(b) Solar panel terminal voltage during high irradiation.
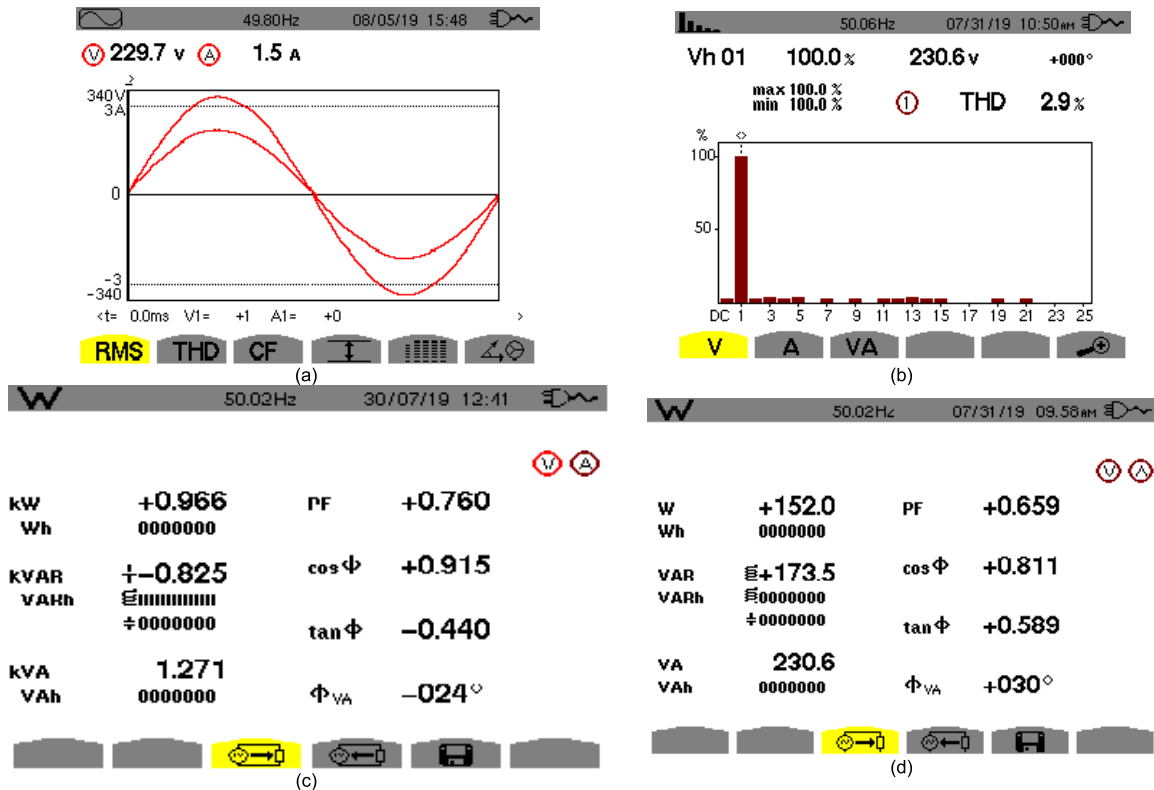
FIGURE 17. (a) RMS Voltage & Current, (b) Voltage THD, (c) AC Power observed during a heavy load condition and (d) AC Power during the lightly loaded condition.

recorded during heavy load and light load conditions and the respective representations are shown in Fig.17 (c) and Fig.17 (d).The personal computers and the other electronic gadgets are connected to sub-buses operating at 12 V using a DC-DC Converters. The output voltage of the solar panel is operated at MPP and fed into the DC bus. A set of four 12 V batteries are connected in series combination to make 48V and it is connected to the DC bus. The solar panel terminals are connected with the MPP converter and it tracks the voltage at which maximum power is attained.

The performance of the battery has been tested with the proposed microgrid and the experimentation is discussed in detail. When charging the battery in the microgrid environment, the conversion process is much reduced and only the bidirectional DC-DC converter is used for charge control. Hence, the conversion losses reduce significantly and the power loss curve is shown in Fig.18. The solar panel, DC loads, and the batteries are connected to the DC bus of the microgrid. The main DC bus voltage of the DC microgrid has been designed to operate at 48 V. The SoC of the battery has been obtained using the open-circuit voltage method and the ESS strategy has been carried out. The SoC of the battery bank used in the proposed system has been obtained using Equation (7) and the respective plot is shown in Fig.19.

FIGURE 18. (a) Power loss during battery charging (b) Power loss during battery discharge in the microgrid environment.

FIGURE 19. SoC of the battery bank of the proposed scheme.

TABLE 3. Solar PV potential [55] and domestic consumer hourly data [56].

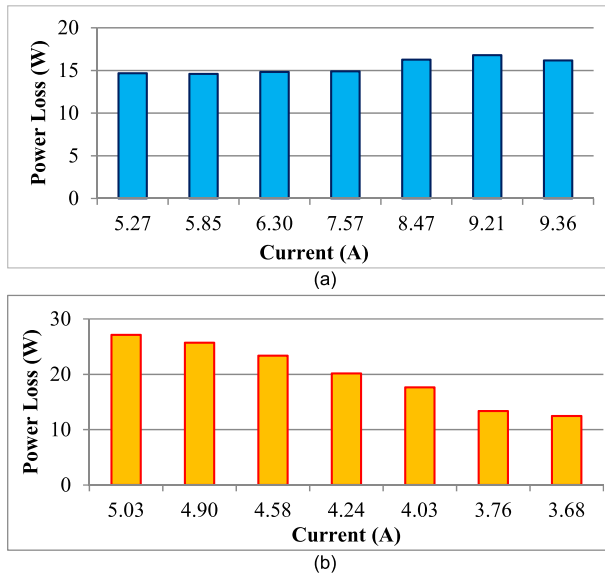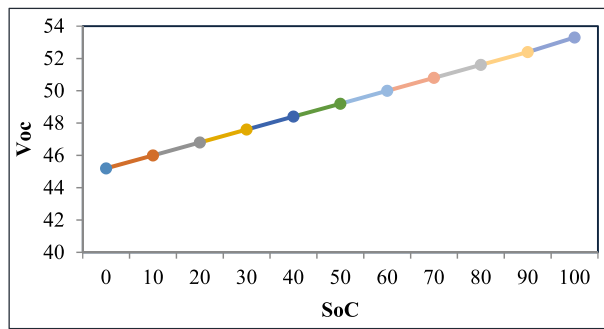| Hours	Ambient Temperature (°C)	Irradiance (W/m²)	DC Array Output (W)	Averaged Hourly Load consumption \day (W)
0	22.244	0	0	384.17
1	21.765	0	0	350.63
2	21.331	0	0	329.79
3	20.965	0	0	329.79
4	20.625	0	0	384.17
5	20.326	0	0	480.21
6	22.105	0	0	762.08
7	25.699	176.492	140.983	864.38
8	28.928	462.707	360.468	868.75
9	31.457	749.333	538.987	956.25
10	33.336	918.126	632.724	960.42
11	34.627	1015.382	706.22	864.38
12	35.253	1037.075	715.193	768.33
13	35.293	975.038	677.895	713.96
14	34.83	830.184	590.165	687.50
15	33.729	624.961	456.195	670.83
16	32.034	381.406	279.857	672.92
17	29.391	144.65	107.653	713.96
18	27.59	0	0	768.33
19	26.339	0	0	734.79
20	25.211	0	0	672.29
21	24.232	0	0	617.92
22	23.496	0	0	521.88
23	22.892	0	0	430.42

TABLE 4. Considerations in the analysis.

Conversion Device	Efficiency	Reference
DC equipment conversion	90%	[46]
Inverter	As per Polynomial relation stated in Eq.(6)	Ref. Fig. 6
AC/DC conversion	90%	[46]
DC/DC conversion	95%	[45]
Battery efficiency in DC environment	95%	[44]

A. REALIZATION OF THE BENEFICIAL CHARACTERISTICS OF THE PROPOSED MICROGRID SCHEME

A detailed residential distribution strategy has been considered for investigation. The solar power potential of the research location is obtained from the NREL database [55] and a load of a domestic consumer hourly data is obtained from the Ref. [56] and the value is averaged for a single home. The solar PV and load data have been depicted in Table-3. The conventional direct grid-tie scheme and existing microgrid scheme have been taken for comparison with the proposed EMS scheme.

The efficiency of the various energy conversion and storage devices is considered based on literature and experimental inferences are depicted in Table-4. An extensive investigation has been carried out to analyze the outcomes of the schemes taken for comparison. The deduced data and results of each scheme are depicted in Appendix 1, 2 & 3.Conversion loss is one of the important criteria which highly affect the performance of the system. Conversion loss is unavoidable when renewable sources are deployed for utilization. In a solar PV

based system, power conversion occurs in various forms in each scheme. Extensive analysis has been carried out and the conversion loss criteria accounted for in each scheme has been investigated and the values have been furnished in Appendix 4 and the respective graph has been depicted in Fig.20. Fig.21 shows a loss comparison chart of the schemes considered for the study. Consecutively, the power driven from the utility by various schemes was depicted in Fig.22.

The deployment of solar PV has resulted in energy saving. Fig.23 shows the energy savings attained by the schemes taken for discussion. The details about the electricity consumption from the utility, conservation of power, and losses are accounted for in the various schemes for a day that have been furnished in Appendix 5.

The energy scenario of various schemes has been deduced for a complete year, detailed in Appendix 6 and a comparative chart of energy-saving, conversion loss, utility power
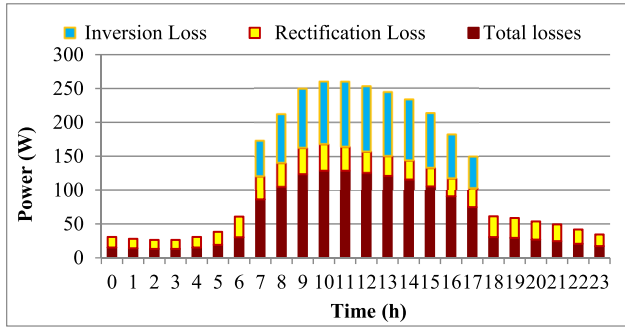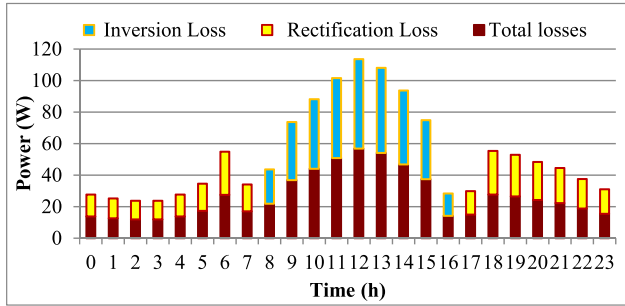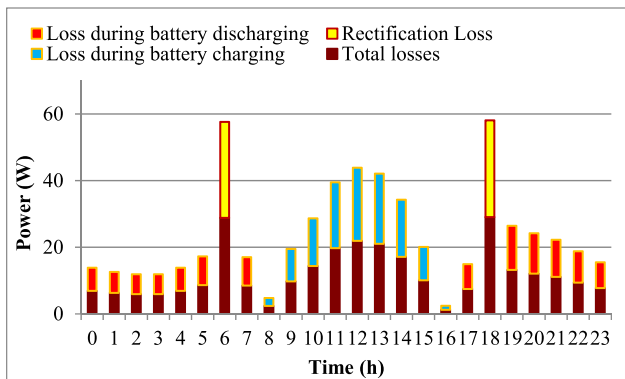
FIGURE 20. Various loss criteria encountered in the schemes/day (a) Direct grid-tied scheme, (b) Conventional microgrid scheme, and (c) Proposed EMS scheme.
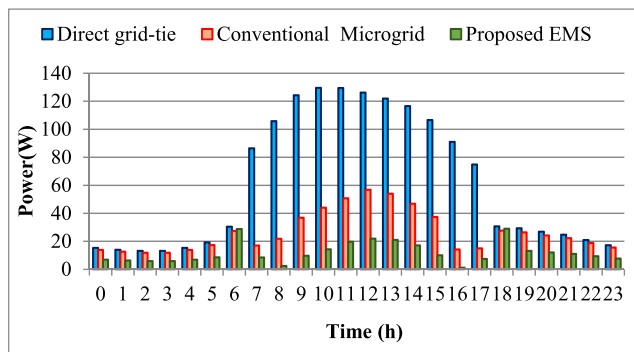
FIGURE 21. Net conversion loss encountered in various schemes, where the proposed EMS is showing the lowest loss.

FIGURE 22. Power consumed from the utility in various schemes.
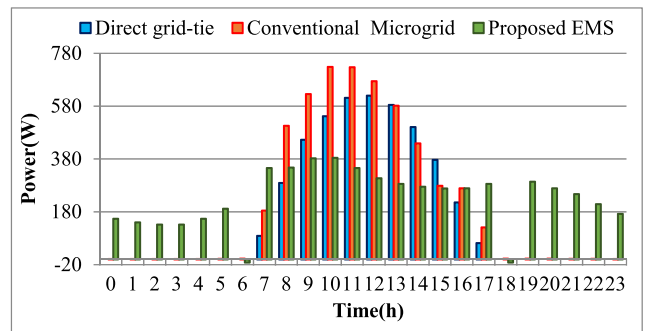
FIGURE 23. Energy savings due to the deployment of solar PV in various schemes.
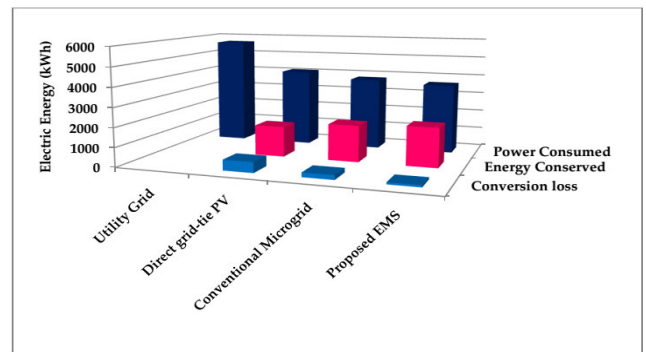
FIGURE 24. Comparison of performance parameters calculated for a year.

TABLE 5. Significance of the proposed scheme comparedwith the existingsolar PV schemes.

S.N	Parameters	Direct Grid-Tie	Conventional Microgrid	Proposed EMS
1	Conversion loss Reduction (kWh/Year)	9.56%	4.11%	1.84%
2	Energy Conserved (kWh/Year)	28.01%	33.28%	35.9%
3	Battery Efficiency	78-83%	82-85%	93-96%

consumption has been depicted in Fig.24. The energy savings are obtained by the incorporation of the proposed scheme (detailed in Table-5). The microgrid enables the utilization of energy-efficient DC loads such as fan, lighting load, and electronic gadgets such as computers, laptop chargers, music systems, TV to be directly get connected to the DC terminal
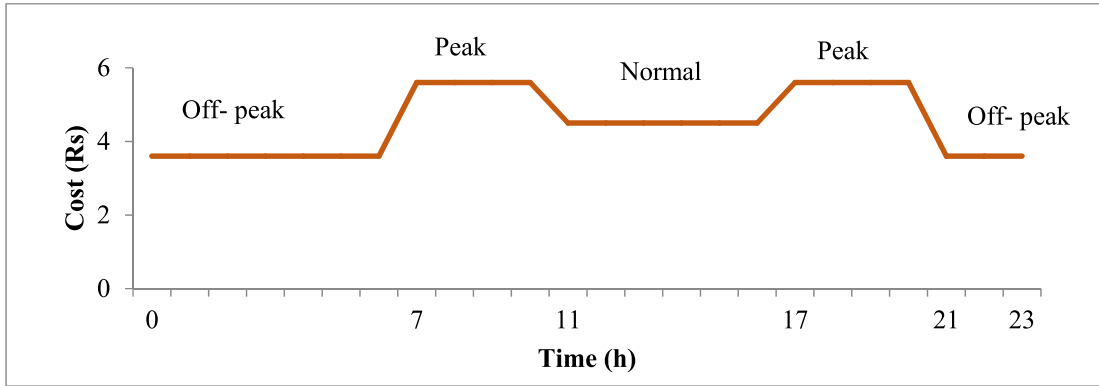
FIGURE 25. Time-of-use rate pattern for a day.
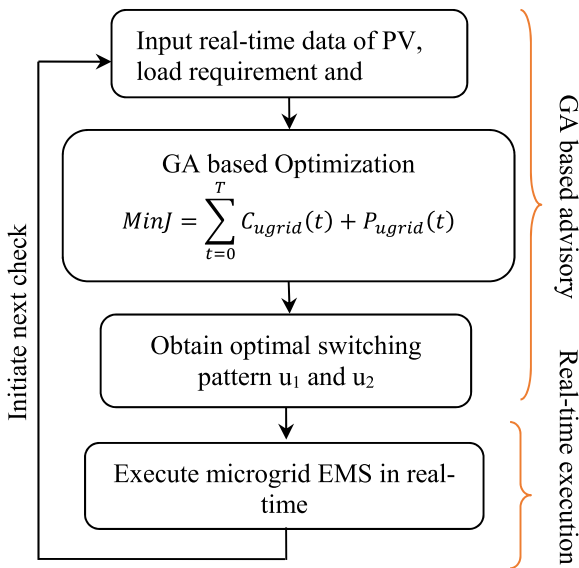
FIGURE 26. Genetic algorithm based microgrid EMS flow chart.

TABLE 6. Energy and cost comparison of various schemes.

Schemes	Net Power Consumed from Utility Grid/Month	Energy Savings due to Solar PV deployment/Month	Electricity Charges/Month
Conventional	465244.5	-	2165.133
Direct Grid-Tied	334937.7	130306.8	1529.987
Conventional Microgrid	310401.9	154842.6	1403.495
GA-EMS	337694.3	153023.7	1260.962

without undergoing major losses and also harmonic issues are eliminated. The generated solar DC power has been utilized to feed DC loads directly and hence frequent power conversion is reduced tremendously. The battery storage system efficiency has been greatly improved in a DC environment.

VIII. COST OPTIMIZATION BASED MICROGRID ENERGY MANAGEMENT USING GENETIC ALGORITHM

Many countries follow the time-of-use tariff for managing the peak demand. In such a location, microgrid energy management requires optimization to attain cost-effective
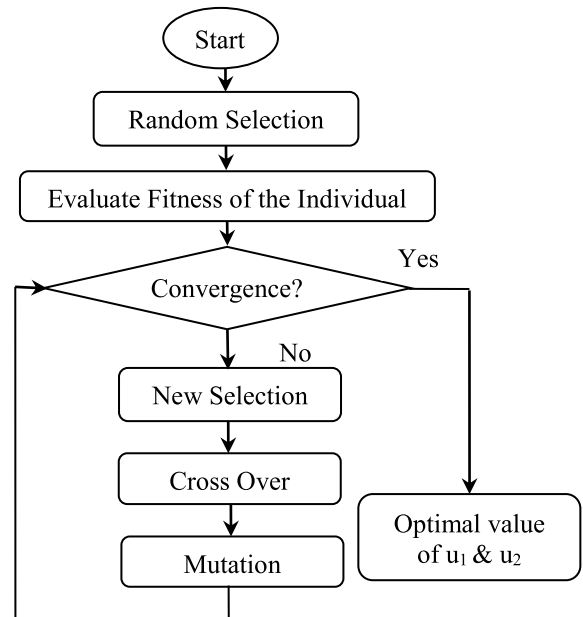
FIGURE 27. Execution of genetic algorithm for optimizing the energy distribution strategy.
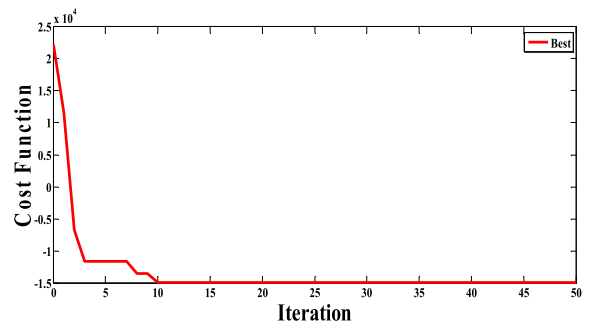
FIGURE 28. The convergence of cost function chart.
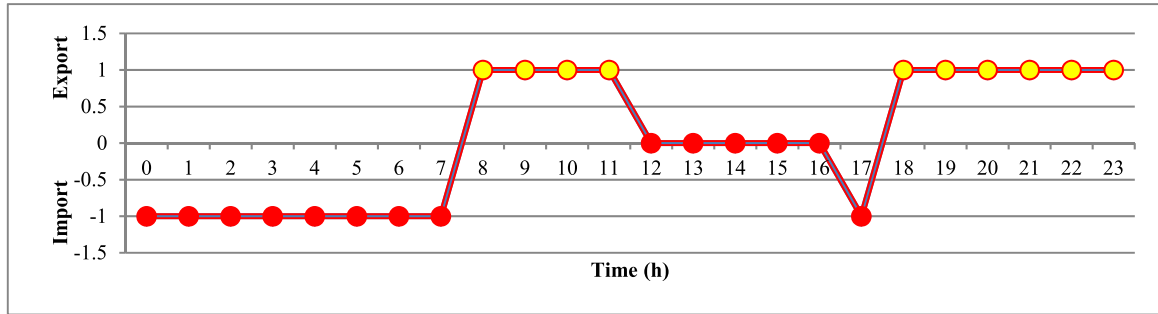
FIGURE 29. Bidirectional interlinking converter invoke switch (S$_U$) operated using the pattern (u$_1$) obtained from GA.
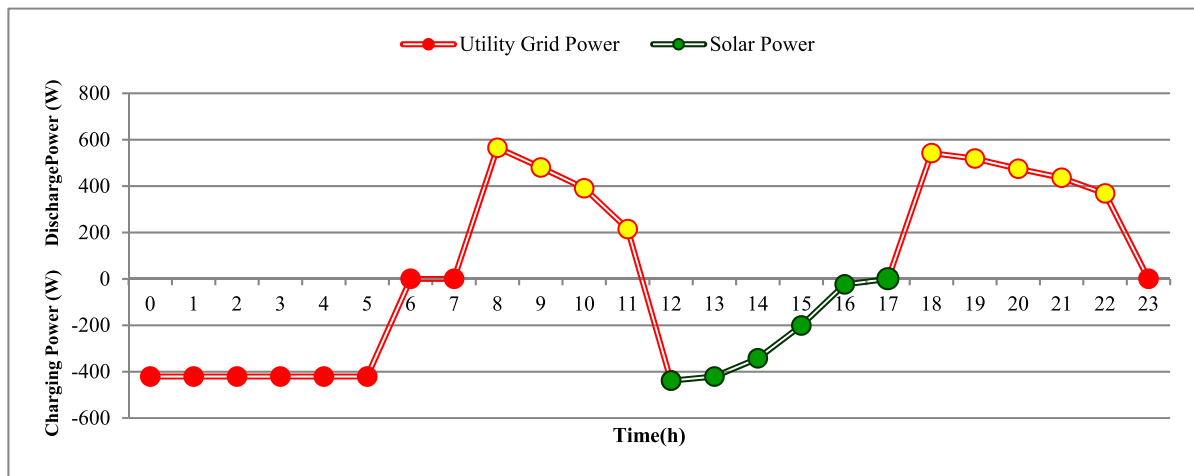
FIGURE 30. Battery management using the switching pattern (u$_2$) obtained from GA.
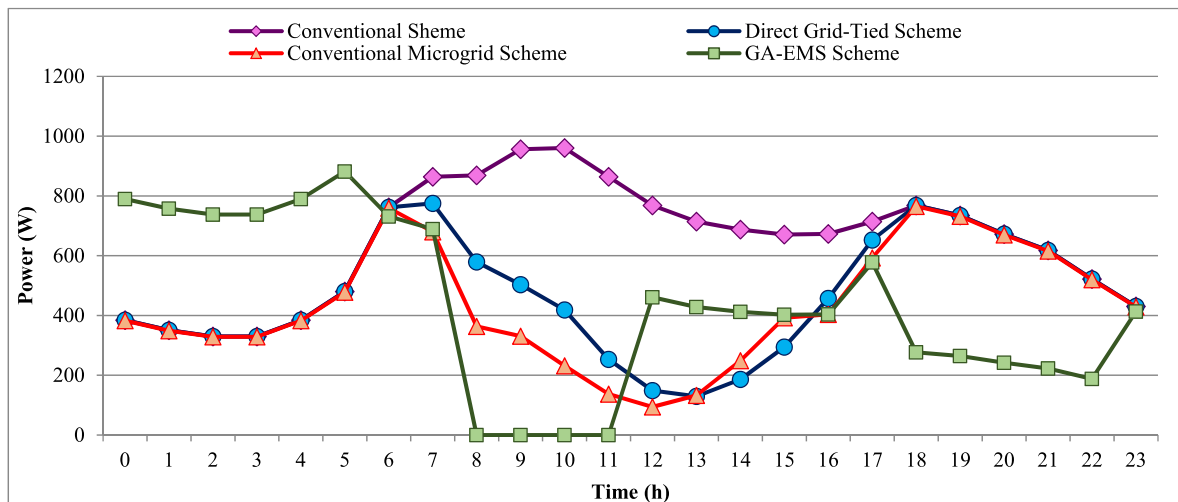
FIGURE 31. Power driven from utility by various schemes.

functionality and also to manage power distribution during peak demand hours. The EMS strategy discussed in Fig.13 is applicable for the region where the flat tariff system is under practice. Though the strategy minimizes the conversion losses, it cannot offer cost-effective operation consistently in places where the time-of-use tariff

system is followed. Hence, it has been proposed to perform a Genetic Algorithm based optimization of microgrid energy management. By this strategy, the power is distributed optimally to attain cost-effective electricity consumption from the utility grid. The steps involved in incorporating the optimization for microgrid energy management in a real-time scenario

TABLE 7. Direct grid-tie scheme.

Hours	1 kW PV Panel DC Array Output (W)	Solar PV current (A)	Inverter efficiency w.r.to power rating (%)	PV power delivered to the utility grid (W)	Loss during Inversion (W)	Averaged Hourly Load consumption \day (W)	AC load consumption (W) – considered as 60% of the Net Power	DC load consumption (W) –Considered 40% of the Net Power	Actual power consumed by DC loads 9W)– excluding loss @ 10%	Loss during DC conversion (W)	Total loss (W)
0	-	-	-	-	-	384.17	230.5	153.67	138.3	15.37	15.37
1	-	-	-	-	-	350.63	210.38	140.25	126.22	14.03	14.03
2	-	-	-	-	-	329.79	197.87	131.92	118.72	13.2	13.2
3	-	-	-	-	-	329.79	197.87	131.92	118.72	13.2	13.2
4	-	-	-	-	-	384.17	230.5	153.67	138.3	15.37	15.37
5	-	-	-	-	-	480.21	288.13	192.08	172.87	19.21	19.21
6	-	-	-	-	-	762.08	457.25	304.83	274.35	30.48	30.48
7	140.98	1.47	63.26	89.18	51.8	864.38	518.63	345.75	311.17	34.58	86.38
8	360.47	3.75	80.3	289.46	71.01	868.75	521.25	347.5	312.75	34.75	105.76
9	538.99	5.61	84.03	452.92	86.06	956.25	573.75	382.5	344.25	38.25	124.31
10	632.72	6.59	85.6	541.59	91.13	960.42	576.25	384.17	345.75	38.42	129.55
11	706.22	7.36	86.56	611.34	94.88	864.38	518.63	345.75	311.17	34.58	129.46
12	715.19	7.45	86.66	619.77	95.43	768.33	461	307.33	276.6	30.73	126.16
13	677.9	7.06	86.23	584.57	93.33	713.96	428.38	285.58	257.02	28.56	121.89
14	590.17	6.15	84.91	501.13	89.03	687.5	412.5	275	247.5	27.5	116.53
15	456.2	4.75	82.51	376.42	79.78	670.83	402.5	268.33	241.5	26.83	106.61
16	279.86	2.92	77.12	215.83	64.03	672.92	403.75	269.17	242.25	26.92	90.95
17	107.65	1.12	56.99	61.35	46.3	713.96	428.38	285.58	257.02	28.56	74.86
18	-	-	-	-	-	768.33	461	307.33	276.6	30.73	30.73
19	-	-	-	-	-	734.79	440.87	293.92	264.53	29.39	29.39
20	-	-	-	-	-	672.29	403.37	268.92	242.03	26.89	26.89
21	-	-	-	-	-	617.92	370.75	247.17	222.45	24.72	24.72
22	-	-	-	-	-	521.88	313.13	208.75	187.87	20.88	20.88
23	-	-	-	-	-	430.42	258.25	172.17	154.95	17.22	17.22
Total	**5206.34**	**54.23**	**874.18**	**4343.56**	**862.78**	**15508.15**	**9304.89**	**6203.26**	**5893.1**	**620.37**	**1483.15**

TABLE 8. Conventional microgrid scheme.

Hours	DC load consumption (W)	AC load consumption (W)	DC array output (W)	Solar DC power after feeding DC load (W)	power required by DC load from AC side (W)	DC load fed by utility (W)	Rectifier loss (W)	Solar power available to transfer after feeding DC load (W)	Solar PV current (A)	Inverter efficiency w.r.to I rating (%)	DC inverted to AC (W)	Inverter loss (W)	Net power consumed from the utility (W)
0	138.3	230.5	-	-138.3	138.3	152.13	13.83	-	-	-	-	-	382.63
1	126.22	210.38	-	-126.22	126.22	138.84	12.62	-	-	-	-	-	349.22
2	118.72	197.87	-	-118.72	118.72	130.59	11.87	-	-	-	-	-	328.46
3	118.72	197.87	-	-118.72	118.72	130.59	11.87	-	-	-	-	-	328.46
4	138.3	230.5	-	-138.3	138.3	152.13	13.83	-	-	-	-	-	382.63
5	172.87	288.13	-	-172.87	172.87	190.16	17.29	-	-	-	-	-	478.29
6	274.35	457.25	-	-274.35	274.35	301.79	27.44	-	-	-	-	-	759.04
7	311.17	518.63	140.98	-170.19	170.19	187.21	17.02	-	-	-	-	-	679.94
8	312.75	521.25	360.47	47.72	-	-	-	47.72	0.99	54.27	25.9	21.82	363.35
9	344.25	573.75	538.99	194.74	-	-	-	194.74	4.06	81.08	157.9	36.84	330.86
10	345.75	576.25	632.72	286.97	-	-	-	286.97	5.98	84.64	242.9	44.08	232.00
11	311.17	518.63	706.22	395.05	-	-	-	395.05	8.238	87.14	344.25	50.80	136.84
12	276.6	461	715.19	438.59	-	-	-	438.59	9.14	87.05	381.79	56.8	94.16
13	257.02	428.38	677.9	420.88	-	-	-	420.88	8.77	87.16	366.84	54.04	132.55
14	247.5	412.5	590.17	342.67	-	-	-	342.67	7.14	86.33	295.83	46.84	248.68
15	241.5	402.5	456.2	214.7	-	-	-	201.28	4.19	81.39	163.82	37.46	392.53
16	242.25	403.75	279.86	37.61	-	-	-	24.15	0.50	41.30	9.97	14.18	403.75
17	257.02	428.38	107.65	-149.37	149.37	164.31	14.94	-	-	-	-	-	592.69
18	276.6	461	-	-276.6	276.6	304.26	27.66	-	-	-	-	-	765.26
19	264.53	440.87	-	-264.53	264.53	290.98	26.45	-	-	-	-	-	731.85
20	242.03	403.37	-	-242.03	242.03	266.23	24.20	-	-	-	-	-	669.60
21	222.45	370.75	-	-222.45	222.45	244.70	22.25	-	-	-	-	-	615.45
22	187.87	313.13	-	-187.87	187.87	206.66	18.79	-	-	-	-	-	519.79
23	154.95	258.25	-	-154.95	154.95	170.45	15.5	-	-	-	-	-	428.7
Total	**5582.89**	**9304.89**	**5206.34**	**-686.76**	**2755.47**	**3031.017**	**275.55**	**2235.63**	**46.58**	**679.09**	**1887.53**	**362.86**	**10346.72**

TABLE 9. Proposed EMS scheme.

Hours	DC load consumption (W)	AC load consumption (W)	DC array output (W)	Power required by DC load excluding PV power (W)	Battery Feeds DC load @ 95% efficiency	Solar current (A)	DC load required from AC side (W)	Utility feed DC loads (W) @ 90%	DC available after feeding DC load (W)	DC power stored in Battery (W) @ 95%	Battery charging loss (W)	Rectifier loss (W)	Battery discharging loss (W)	Net power consumed from the utility (W)
0	138.3	230.5	-	138.3	145.22	3.025	-	-	-	-	-	-	6.92	230.5
1	126.22	210.38	-	126.22	132.53	2.76	-	-	-	-	-	-	6.31	210.38
2	118.72	197.87	-	118.72	124.66	2.6	-	-	-	-	-	-	5.94	197.87
3	118.72	197.87	-	118.72	124.66	2.6	-	-	-	-	-	-	5.94	197.87
4	138.3	230.5	-	138.3	145.22	3.03	-	-	-	-	-	-	6.92	230.5
5	172.87	288.13	-	172.87	181.51	3.78	-	-	-	-	-	-	8.64	288.13
6	274.35	457.25	-	274.35	-	6.00	288.07	316.87	-	-	-	28.80	-	774.12
7	311.17	518.63	140.98	170.19	178.7	3.72	-	-	-	-	-	-	8.51	518.63
8	312.75	521.25	360.47	-	-	-	-	-	47.72	45.33	2.39	-	-	521.25
9	344.25	573.75	538.99	-	-	-	-	-	194.74	185.00	9.74	-	-	573.75
10	345.75	576.25	632.72	-	-	-	-	-	286.97	272.62	14.35	-	-	576.25
11	311.17	518.63	706.22	-	-	-	-	-	395.05	375.3	19.75	-	-	518.63
12	276.6	461	715.19	-	-	-	-	-	438.59	416.66	21.93	-	-	461.00
13	257.02	428.38	677.9	-	-	-	-	-	420.88	399.84	21.04	-	-	428.38
14	247.5	412.5	590.17	-	-	-	-	-	342.67	325.54	17.13	-	-	412.5
15	241.5	402.5	456.2	-	-	-	-	-	201.28	191.22	10.06	-	-	402.5
16	242.25	403.75	279.86	-	-	-	-	-	24.15	22.94	1.21	-	-	403.75
17	257.02	428.38	107.65	149.37	156.84	3.27	-	-	-	-	-	-	7.47	428.38
18	276.6	461	-	276.6	-	6.05	290.43	319.47	-	-	-	29.04	-	780.47
19	264.53	440.87	-	264.53	277.76	5.79	-	-	-	-	-	-	13.22	440.87
20	242.03	403.37	-	242.03	254.13	5.29	-	-	-	-	-	-	12.10	403.37
21	222.45	370.75	-	222.45	233.57	4.87	-	-	-	-	-	-	11.12	370.75
22	187.87	313.13	-	187.87	197.26	4.11	-	-	-	-	-	-	9.39	313.13
23	154.95	258.25	-	154.95	162.70	3.39	-	-	-	-	-	-	7.75	258.25
Total	5582.89	9304.89	5206.34	2755.47	2314.75	60.28	578.5	636.343	2352.05	1887.53	117.60	57.85	110.23	9941.23

■ **Note:** The red color marked columns are feeble power values prevailing in the microgrid system.

TABLE 10. Losses accounted in various PV schemes.

Direct grid-tie scheme

Hours	Loss during Inversion (W)	Loss during Rectification (W)	Total losses
0	-	15.37	15.37
1	-	14.03	14.03
2	-	13.2	13.2
3	-	13.2	13.2
4	-	15.37	15.37
5	-	19.21	19.21
6	-	30.48	30.48
7	51.8	34.58	86.38
8	71.01	34.75	105.76
9	86.06	38.25	124.31
10	91.13	38.42	129.55
11	94.88	34.58	129.46
12	95.43	30.73	126.16
13	93.33	28.56	121.89
14	89.03	27.5	116.53
15	79.78	26.83	106.61
16	64.03	26.92	90.95
17	46.3	28.56	74.86
18	-	30.73	30.73
19	-	29.39	29.39
20	-	26.89	26.89
21	-	24.72	24.72
22	-	20.88	20.88
23	-	17.22	17.22
Total	862.78	620.37	1483.15

Conventional microgrid scheme

Hours	Loss during Rectification (W)	Loss during Inversion (W)	Total losses
0	13.83	-	13.83
1	12.62	-	12.62
2	11.87	-	11.87
3	11.87	-	11.87
4	13.83	-	13.83
5	17.29	-	17.29
6	27.44	-	27.44
7	17.02	-	17.02
8	-	21.82	21.82
9	-	36.85	36.84
10	-	44.079	44.08
11	-	50.80343	50.80
12	-	56.8	56.8
13	-	54.04	54.04
14	-	46.84	46.84
15	-	37.46	37.46
16	-	14.18	14.18
17	14.94	-	14.94
18	27.66	-	27.66
19	26.45	-	26.45
20	24.20	-	24.20
21	22.25	-	22.25
22	18.787	-	18.79
23	15.495	-	15.5
Total	275.55	362.86	638.41

Proposed EMS scheme

Hours	Loss during battery charging (W)	Loss during Rectification (W)	Loss during discharging (W)	Total losses (W)
0	-	-	6.92	6.92
1	-	-	6.31	6.31
2	-	-	5.94	5.94
3	-	-	5.94	5.94
4	-	-	6.92	6.92
5	-	-	8.64	8.64
6	-	28.80	-	28.80
7	-	-	8.51	8.51
8	2.39	-	-	2.39
9	9.74	-	-	9.74
10	14.35	-	-	14.35
11	19.75	-	-	19.75
12	21.93	-	-	21.93
13	21.04	-	-	21.04
14	17.13	-	-	17.13
15	10.06	-	-	10.06
16	1.21	-	-	1.21
17	-	-	7.47	7.47
18	-	29.04	-	29.04
19	-	-	13.22	13.22
20	-	-	12.10	12.10
21	-	-	11.12	11.12
22	-	-	9.39	9.39
23	-	-	7.75	7.75
Total	117.60	57.85	110.23	285.65

TABLE 11. Electricity consumption from the utility, conservation of power and losses accounted for various schemes for a day.

Hours	Utility Consumption (W)/day				Conservation (W)/day			Losses (W)/day		
	Averaged hourly Load consumption \day	Direct grid-tie	Conventional Microgrid	Proposed EMS	Direct grid-tie	Conventional Microgrid	Proposed EMS	Direct grid-tie	Conventional Microgrid	Proposed EMS
0	384.17	384.17	382.63	230.5	-	1.54	153.67	15.37	13.83	6.92
1	350.63	350.63	349.222	210.38	-	1.408	140.25	14.03	12.62	6.31
2	329.79	329.79	328.462	197.87	-	1.328	131.92	13.2	11.87	5.94
3	329.79	329.79	328.462	197.87	-	1.328	131.92	13.2	11.87	5.94
4	384.17	384.17	382.63	230.5	-	1.54	153.67	15.37	13.83	6.92
5	480.21	480.21	478.287	288.13	-	1.923	192.08	19.21	17.29	8.64
6	762.08	762.08	759.035	774.12	-	3.045	-12.04	30.48	27.44	28.80
7	864.38	775.2	679.9414	518.63	89.18	184.44	345.75	86.38	17.02	8.51
8	868.75	579.29	363.3548	521.25	289.46	505.4	347.5	105.76	21.82	2.39
9	956.25	503.33	330.8586	573.75	452.92	625.4	382.5	124.31	36.85	9.74
10	960.42	418.83	232.0034	576.25	541.59	728.42	384.17	129.55	44.08	14.35
11	864.38	253.04	136.8374	518.63	611.34	727.54	345.75	129.46	50.80	19.75
12	768.33	148.56	94.161	461	619.77	674.17	307.33	126.16	56.8	21.93
13	713.96	129.39	132.553	428.38	584.57	581.41	285.58	121.89	54.04	21.04
14	687.5	186.37	248.6782	412.5	501.13	438.82	275	116.53	46.84	17.13
15	670.83	294.41	392.5261	402.5	376.42	278.30	268.33	106.61	37.46	10.06
16	672.92	457.09	403.75	403.75	215.83	269.17	269.17	90.95	14.18	1.21
17	713.96	652.61	592.687	428.38	61.35	121.27	285.58	74.86	14.94	7.47
18	768.33	768.33	765.26	780.473	-	3.07	-12.143	30.73	27.66	29.04
19	734.79	734.79	731.853	440.87	-	2.94	293.92	29.39	26.45	13.22
20	672.29	672.29	669.603	403.37	-	2.69	268.92	26.89	24.20	12.10
21	617.92	617.92	615.445	370.75	-	2.48	247.17	24.72	22.25	11.12
22	521.88	521.88	519.787	313.13	-	2.09	208.75	20.88	18.79	9.39
23	430.42	430.42	428.695	258.25	-	1.73	172.17	17.22	15.5	7.75
Total	15508.15	11164.59	10346.72	9941.23	4343.56	5161.43	5566.92	1483.15	638.42	285.65

has been illustrated using the Fig.26. The real-time realization of optimization of microgrid energy management comprises of the following steps:

A. INPUT PROFILES

The optimizer input information comprises of the following information:

a) The AC and DC load power consumption details.
b) Power generated by the solar PV system.
d) Battery SoC and capacity.
c) Daily utility grid electricity time-of-use rate profile, it is shown in Fig.25.

B. OBJECTIVE FUNCTION AND CONSTRAINTS

The objective function of the proposed scheme is to optimize the operating cost of the system by regulating the PV, battery and utility power sources and also by reducing the redundant conversion losses. The operational cost for the grid power is calculated based on an electricity time-of-use rate profile.

In many countries, the residential renewable generation system is not given any revenue and hence the cost of renewable power is assumed to be zero. The cost for the battery power is zero since the charging cost is included in the utility grid power cost. In this regard, the objective function can be stated as

$$Min \; J = \sum_{t=0}^{T} C_{ugrid}(t) * P_{ugrid}(t) \qquad (13)$$

$$P_{ugrid}(t) = P_{ACL}(t) + P_{inv}u_1 - P_{PV}(t) + P_{DCL}(t)$$
$$+ P_{BC}(t) u_2 \qquad (14)$$

where $u_1 = \begin{cases} 1 & import\,or\,export\;power \\ 0 & off\;state \end{cases}$

u_1 is the pattern with which the bidirectional interlinking converter is invoked to import or export power during energy distribution management.

$$u_2 = \begin{cases} 1 & Charging\,mode, S_1 \; and \; D_2 \; conducts \\ 0 & Float\,mode\,using\,triggle\,charging \\ -1 & Discharging\,mode, S_2 \; and \; D_1 \; conducts \end{cases}$$

u_2 is the switching strategy of the bidirectional DC/DC converter shown in Figure.9. The u_2 operates with the SoC of the battery as a reference. The SoC of the battery is obtained using the expression as shown.

$$SoC = \left(1 - \frac{1}{Q} \int I_B dt\right) \qquad (15)$$

The constraints used in the system are as follows:

- $SoC(t)^{min} > 50\%$
- $SoC(t)^{max} < 90\%$
- $P_N > 20\% of \; P_{int-conv}$
- $P_{DCL} > 75\% of \; DC\,load\,requirement$

C. EXECUTING GA EMPLOYING THE SWITCHING STRATEGY

The flow chart for executing the genetic algorithm is shown in Fig.27. It is used to optimize the electricity cost by

TABLE 12. Comparison of energy managing parameters.

Schemes	Power Consumed from the utility (kWh/Year)	Conversion loss (kWh/year)	Energy Conserved (kWh/Year)
Conventional scheme	5660.48	-	-
Direct grid-tie PV	4075.08	541.35	1585.40
Conventional microgrid	3776.55	233.02	1883.92
Proposed EMS	3628.55	104.26	2031.93

minimizing the power consumed from the utility grid. The execution of GA comprises the following steps:

- Random selection of population (population size=60).
- Evaluation of fitness of the individual.
- Check if satisfy criterion is attained.
- If not another set of new populations is selected. The roulette wheel selection strategy is used for the selection process.
- Cross over is carried out. Single cross over is done in this scheme.
- The mutation rate is fixed at 0.15.
- Again the process is iterated and checked if the output has attained the convergence.
- The converged output value is used for real-time control.

D. ADVISORY CONTROL OUTPUT

Executing the genetic algorithm resulted in a convergence of cost function, it is shown in Fig.28.

The best fit switching patterns for u1 and u2 have been received using GA optimization and it is depicted as follows:

$$u_1 = \begin{bmatrix} -1-1-1-1-1-1-1-1 \\ 111100000-11111 \end{bmatrix}$$

$$u_2 = \begin{bmatrix} -1-1-1-1-1-100111 \\ 1-1-1-1-1-101111 \end{bmatrix}$$

The switching pattern has been used to perform microgrid energy management. The pattern u_1 for converter operation is obtained as in Fig.29. The battery energy management strategy using the obtained pattern u_2 has been shown in Fig.30. The pattern played a significant role in drawing power from utility at minimal cost satisfying the defined constraints. The comparison chart of the energy consumed from the utility grid has been depicted in Fig. 31. The cost of electricity in various schemes has been furnished in Table-6. The proposed scheme shows a reduced cost and effective energy savings.

IX. CONCLUSION

An extensive qualitative and quantitative experimental result analysis has been carried out to identify the detrimental factors of the conventional distribution system. A novel hybrid

microgrid energy management technology has been incorporated to enhance the residential power distribution system by reducing the conversion processes. The solar PV equipped hybrid AC/DC microgrid model has been designed and validated. A prototype hardware setup has been developed and tested in the laboratory to illustrate the significance of the proposed strategy. The conversion loss reduction strategy has been accomplished using the automatic centralized microgrid controller and accomplished energy management effectively. A comparative analysis has been carried out to demonstrate the effectiveness of the proposed scheme with the existing technologies. The implementation of the proposed distribution system has resulted in the following beneficial accomplishments:

- The feeble power has been managed effectively and conversion losses have been reduced significantly.
- Effective battery supported energy management has resulted in the reduction of multiple conversion processes and battery energy efficiency has been improved by 8-10%.
- The intellectual management of renewable resources, BESS, and the demand response has resulted in the improved energy economy.
- Optimized the energy utilization in the microgrid environment using a genetic algorithm and cost of the electricity has been reduced significantly.

ABBREVIATIONS

AC	Alternating Current
ACMC	Automatic Centralized Microgrid Controller
BESS	Battery Energy Storage Systems
C_AAC	side filter capacitor
C_DDC	side filter capacitor
DC	Direct Current
E_{lp}	Leakage inductance in the primary of the transformer
EMS	Energy Management System
E_{off}	Energy loss during turning OFF of IGBT
E_{on}	Energy loss during turning ON of IGBT
f_{sw}	Switching Frequency
I_{AC}	Current in the AC bus
I_{ce}	Collector to emitter Current of the IGBT switch
I_{DCL}	DC load current
IGBT	Insulated Gate Bipolar Transistor
I_{nom}	Nominal Current
I_{pk}	Peak current
I_{PV}	Current flow from the solar PV panel
L_A	AC side filter inductor
L_l	Line inductance
L_{tr}	Transformer leakage inductance
MPPT	Maximum Power Point Tracking
P_{ACL}	Power drawn by AC loads
P_{BC}	Battery Charging Power
$P_{chg,loss}$	Battery Charging loss
$P_{d.cond,loss}$	Conduction loss in diode

$P_{dcond,loss}$	Loss during the reverse recovery of the diode
$P_{dc.conv,loss}$	DC-DC Converter Loss
P_{DCL}	Power drawn by DC loads
$P_{diode,loss}$	Diode loss
$P_{dis,loss}$	Battery discharging loss
$P_{IGBT.Cond}$	Total conduction loss in IGBT
$P_{int,loss}$	Battery internal loss
$P_{inv,loss}$	Inverter Loss
P_N	Net Power at DC Side
P_{PV}	Power from PV array
$P_{rec,loss}$	Rectifier Loss
$P_{Conv,loss}$	Power conversion loss
$P_{sw,loss}$	Switching power loss
$P_{batt,loss}$	Power loss in battery
V_{OC}	Open circuit voltage
I_{SC}	Short circuit current
V_{MP}	Maximum power point tracking voltage
I_{MP}	Maximum power point tracking current
$P_{SW.IGBT}$	Total switching loss in IGBT
$P_{trs,loss}$	Transformer Loss
PV	Photo Voltaic
PWM	Pulse Width Modulation
S_C	Converter connect switch
SoC	State of Charge
S_U	Utility connect switch
THD	Total Harmonic Distortion
Unit	one unit is 1kWh
V_{ce}	Collector to emitter voltage of the IGBT switch
V_{dc}	DC Voltage
V_g	Grid voltage
V_{nom}	Nominal Voltage
V_{PV}	Voltage across the solar panel

APPENDIX I. DIRECT GRID-TIE SCHEME
See Table 7.

APPENDIX II. CONVENTIONAL MICROGRID SCHEME
See Table 8.

APPENDIX III. PROPOSED EMS SCHEME
See Table 9.

APPENDIX IV. LOSSES ACCOUNTED IN VARIOUS PV SCHEMES
See Table 10.

APPENDIX V. ELECTRICITY CONSUMPTION FROM THE UTILITY, CONSERVATION OF POWER AND LOSSES ACCOUNTED FOR VARIOUS SCHEMES FOR A DAY
See Table 11.

APPENDIX VI. COMPARISON OF ENERGY MANAGING PARAMETERS
See Table 12.

ACKNOWLEDGMENT

REFERENCES

[1] M. A. Rodriguez-Otero and E. O'Neill-Carrillo, "Efficient home appliances for a future DC residence," in *Proc. IEEE Energy Conf.*, Nov. 2008, pp. 17–18, doi: 10.1109/ENERGY.2008.4781006.

[2] S. Foster Porter, D. Denkenberger, S. Mercier, and P. May-Ostendorp, "Reviving the war of currents: Opportunities to save energy with DC distribution in commercial buildings," in *Proc. ACEEE Summer Study Energy Efficiency Buildings*, Aug. 2014, vol. 85, p. 3. [Online] Available:https://www.researchgate.net/publication/281210054

[3] R. Bayindir, E. Hossain, E. Kabalci, and R. Perez, "A comprehensive study on microgrid technology," *Int. J. Renew. Energy Res.*, vol. 4, no. 4, Dec. 2014, Art. no. 4.

[4] M. S. Mahmoud, *Microgrid Advanced Control Methods and Renewable Energy System Integration*, vol. 1. Amsterdam, The Netherlands: Elsevier, 2017, pp. 1–42.

[5] A. Hirsch, Y. Parag, and J. Guerrero, "Microgrids: A review of technologies, key drivers, and outstanding issues," *Renew. Sustain. Energy Rev.*, vol. 90, pp. 402–411, Jul. 2018.

[6] M. F. Zia, E. Elbouchikhi, and M. Benbouzid, "Microgrids energy management systems: A critical review on methods, solutions, and prospects," *Appl. Energy*, vol. 222, pp. 1033–1055, Jul. 2018.

[7] Y. Wang, Z. Sun, and Z. Chen, "Development of energy management system based on a rule-based power distribution strategy for hybrid power sources," *Energy*, vol. 175, pp. 1055–1066, May 2019.

[8] E. Hossain, H. M. R. Faruque, M. S. H. Sunny, N. Mohammad, and N. Nawar, "A comprehensive review on energy storage systems: Types, comparison, current scenario, applications, barriers, and potential solutions, policies, and future prospects," *Energies*, vol. 13, no. 14, p. 3651, Jul. 2020.

[9] H. Shayeghi, E. Shahryari, M. Moradzadeh, and P. Siano, "A survey on microgrid energy management considering flexible energy sources," *Energies*, vol. 12, pp. 1–26, Jun. 2019.

[10] P. S. Kumar, R. P. S. Chandrasena, V. Ramu, G. N. Srinivas, and K. V. S. M. Babu, "Energy management system for small scale hybrid wind solar battery based microgrid," *IEEE Access*, vol. 8, pp. 8336–8345, 2020.

[11] A. A. Mamun, M. Sohel, N. Mohammad, M. S. Haque Sunny, D. R. Dipta, and E. Hossain, "A comprehensive review of the load forecasting techniques using single and hybrid predictive models," *IEEE Access*, vol. 8, pp. 134911–134939, 2020, doi: 10.1109/ACCESS.2020.3010702.

[12] Zaheeruddin and M. Manas, "Renewable energy management through microgrid central controller design: An approach to integrate solar, wind and biomass with battery," *Energy Rep.*, vol. 1, pp. 156–163, Nov. 2015.

[13] L. Xu and D. Chen, "Control and operation of a DC microgrid with variable generation and energy storage," *IEEE Trans. Power Del.*, vol. 26, no. 4, pp. 2513–2522, Oct. 2011.

[14] K. Venkatraman, B. Dastagiri Reddy, M. P. Selvan, S. Moorthi, N. Kumaresan, and N. A. Gounden, "Online condition monitoring and power management system for standalone micro-grid using FPGAs," *IET Gener., Transmiss. Distrib.*, vol. 10, no. 15, pp. 3875–3884, Nov. 2016.

[15] L. Xiong, P. Li, Z. Wang, and J. Wang, "Multi-agent based multiobjective renewable energy management for diversified community power consumers," *Appl. Energy.*, vol. 259, pp. 114–140, Nov. 2019.

[16] P. Li, D. Xu, Z. Zhou, W.-J. Lee, and B. Zhao, "Stochastic optimal operation of microgrid based on chaotic binary particle swarm optimization," *IEEE Trans. Smart Grid*, vol. 7, no. 1, pp. 66–73, Jan. 2016.

[17] G. Notton and K. Kaldellis, "Hybrid wind-photovoltaic energy systems," in *Stand-Alone and Hybrid Wind Energy Systems*. Amsterdam, The Netherlands: Elsevier, 2010, pp. 216–253.

[18] M. Saad Bin Arif and M. AsifHasan, *Hybrid-Renewable Energy Systems in Microgrids*. Chicago, IL, USA: Woodhead, 2018, pp. 23–37.

[19] Y. Zhang, A. Lundblad, P. E. Campana, F. Benavente, and J. Yan, "Battery sizing and rule-based operation of grid-connected photovoltaic-battery system: A case study in sweden," *Energy Convers. Manage.*, vol. 133, pp. 249–263, Feb. 2017.

[20] P. B. L. Neto, O. R. Saavedra, and L. A. de Souza Ribeiro, "A dual-battery storage bank configuration for isolated microgrids based on renewable sources," *IEEE Trans. Sustain. Energy*, vol. 9, no. 4, pp. 1618–1626, Oct. 2018.

[21] M. El-Hendawi, H. A. Gabbar, G. El-Saady, and E.-N. A. Ibrahim, "Optimal operation and battery management in a grid-connected microgrid," *J. Int. Council Electr. Eng.*, vol. 8, no. 1, pp. 195–206, Oct. 2018, doi: 10.1080/22348972.2018.1528662.

[22] T. M. Masaud and E. F. El-Saadany, "Correlating optimal size, cycle life estimation, and technology selection of batteries: A two-stage approach for microgrid applications," *IEEE Trans. Sustain. Energy*, vol. 11, no. 3, pp. 1257–1267, Jul. 2020.

[23] M. Alramlawi and P. Li, "Design optimization of a residential PV-battery microgrid with a detailed battery lifetime estimation model," *IEEE Trans. Ind. Appl.*, vol. 56, no. 2, pp. 2020–2030, Mar. 2020.

[24] T. Morstyn, A. V. Savkin, B. Hredzak, and V. G. Agelidis, "Multi-agent sliding mode control for state of charge balancing between battery energy storage systems distributed in a DC microgrid," *IEEE Trans. Smart Grid*, vol. 9, no. 5, pp. 4735–4743, Sep. 2018.

[25] H. Mahmood and J. Jiang, "Autonomous coordination of multiple PV/Battery hybrid units in islanded microgrids," *IEEE Trans. Smart Grid*, vol. 9, no. 6, pp. 6359–6368, Nov. 2018.

[26] J.-O. Lee, Y.-S. Kim, T.-H. Kim, and S.-I. Moon, "Novel droop control of battery energy storage systems based on battery degradation cost in islanded DC microgrids," *IEEE Access*, vol. 8, pp. 119337–119345, 2020.

[27] Y. Karimi, H. Oraee, M. S. Golsorkhi, and J. M. Guerrero, "Decentralized method for load sharing and power management in a PV/Battery hybrid source islanded microgrid," *IEEE Trans. Power Electron.*, vol. 32, no. 5, pp. 3525–3535, May 2017.

[28] H. Mahmood and J. Jiang, "Decentralized power management of multiple PV, battery, and droop units in an Islanded microgrid," *IEEE Trans. Smart Grid*, vol. 10, no. 2, pp. 1898–1906, Mar. 2019, doi: 10.1109/TSG.2017.2781468.

[29] B. Glasgo, I. L. Azevedo, and C. Hendrickson, "How much electricity can we save by using direct current circuits in homes? Understanding the potential for electricity savings and assessing feasibility of a transition towards DC powered buildings," *Appl. Energy*, vol. 180, pp. 66–75, Oct. 2016.

[30] *Germany Announces 50m Solar Storage Incentive*. Accessed: Mar. 5, 2019. [Online] Available:https://energystorageforum.com/news/germany-announces-e50m-solar-storage-incentive.

[31] *Italy Extends Fiscal Incentive for Residential PV to Storage*. Accessed: Mar. 8, 2019. [Online] Available:https://www.pv-magazine.com/2018/09/21/italy-extends-storage-fiscal-incentive-for-residential-pv-linked-to-sustainable-buildings/

[32] *Domestic Batteries Best Practice Guide—Learnings From NEA's Technical Innovation Fund Field Trials*. Accessed: Mar. 27, 2019. [Online]. Available: http://www.nea.org.uk/wp-content/uploads/2019/02/Best-Practice-Domestic-Batteries-FINAL-27-03-2019.pdf

[33] *Best Practices for Operation and Maintenance of Photovoltaic and Energy Storage Systems*. Accessed: Apr. 5, 2019. [Online]. Available: https://www.nrel.gov/docs/fy19osti/73822.pdf

[34] R. Elavarasan, G. Shafiullah, N. Manoj Kumar, and S. Padmanaban, "A state-of-the-art review on the drive of renewables in gujarat, state of india: Present situation, barriers and future initiatives," *Energies*, vol. 13, no. 1, p. 40, Dec. 2019.

[35] R. M. Elavarasan, "Comprehensive review on India's growth in renewable energy technologies in comparison with other prominent renewable energy based countries," *J. Sol. Energy Eng.*, vol. 142, no. 3, pp. 030801–030811, Dec. 2019.

[36] R. M. Elavarasan, "The motivation for renewable energy and its comparison with other energy sources: A review," *Eur. J. Sustain. Develop. Res.*, vol. 3, no. 1, pp. 1–19, Feb. 2019.

[37] U. B. Tayab, F. Yang, M. El-Hendawi, and J. Lu, "Energy management system for a grid-connected microgrid with photovoltaic and battery energy storage system," in *Proc. Austral. New Zealand Control Conf. (ANZCC)*, Dec. 2018, pp. 141–144, doi: 10.1109/ANZCC.2018.8606557.

[38] X. Tan, Q. Li, and H. Wang, "Advances and trends of energy storage technology in microgrid," *J. Electr. Power Energy Syst.*, vol. 44, pp. 179–191, Jan. 2013.

[39] Y. Levron, J. M. Guerrero, and Y. Beck, "Optimal power flow in microgrids with energy storage," *IEEE Trans. Power Syst.*, vol. 28, no. 3, pp. 3226–3234, Aug. 2013.

[40] M. E. Baran and I. M. El-Markabi, "A multiagent-based dispatching scheme for distributed generators for voltage support on distribution feeders," *IEEE Trans. Power Syst.*, vol. 22, no. 1, pp. 52–59, Feb. 2007.

[41] C. Colson, M. Nehrir, and C. Wang, "Ant colony optimization for microgrid multi-objective power management power systems conference and exposition," in *Proc. IEEE/PES Power Syst. Conf. Expo.*, pp. 15–18, Mar. 2009.

[42] R. A. Salas-Puente, S. Marzal, R. González-Medina, E. Figueres, and G. Garcera, "Power Management of the DC Bus Connected Converters in a Hybrid AC/DC Microgrid Tied to the Main Grid," *Energies*, vol. 11, pp. 1–22, Mar. 2018.

[43] N. K. Noyanbayev, A. J. Forsyth, and T. Feehally, "Efficiency analysis for a grid-connected battery energy storage system," *Mater. Today, Process.*, vol. 5, no. 11, pp. 22811–22818, 2018.

[44] R. Padbury and X. Zhang, "Lithium–oxygen batteries—Limiting factors that affect performance," *J. Power Sources*, vol. 196, no. 10, pp. 4436–4444, May 2011.

[45] Y. Qin, Y. Yang, S. Li, Y. Huang, S.-C. Tan, and S. Y. Hui, "A high-efficiency DC/DC converter for high-voltage-gain, high-current applications," *IEEE J. Emerg. Sel. Topics Power Electron.*, vol. 8, no. 3, pp. 2812–2823, Sep. 2020, doi: 10.1109/JESTPE.2019.2908416.

[46] *Solar-Facts Charging and Discharging Lead Acid Batteries.* Accessed: Feb. 12, 2020. [Online]. Available: https://www.solar-facts.com/batteries/battery-charging.php.

[47] *Dynex Power Control Through Innovation, Calculating Power Losses in an IGBT Module.* Accessed: Sep. 1, 2014. [Online]. Available: https://www.dynexsemi.com/assets/downloads/DNX_AN6156.pdf

[48] W.-Y. Chang, "The state of charge estimating methods for battery: A review," *ISRN Appl. Math.*, vol. 2013, pp. 1–7, Dec. 2013, doi: 10.1155/2013/953792.

[49] P. Lin, P. Wang, J. Xiao, C. Jin, J. Wang, and K. L. Hai, "Power management of multi-paralleled bidirectional interlinking converters in hybrid AC/DC microgrids: A dynamic consensus approach," in *Proc. Asian Conf. Energy, Power Transp. Electrific. (ACEPT)*, Oct. 2018, pp. 1–5.

[50] W. Li, X. Mou, Y. Zhou, and C. Marnay, "On voltage standards for DC home microgrids energized by distributed sources," in *Proc. 7th Int. Power Electron. Motion Control Conf. (IPEMC)*, Jun. 2012, vol. 3, pp. 2282–2286.

[51] S. Anand and B. G. Fernandes, "Optimal voltage level for DC microgrids," in *Proc. 36th Annu. Conf. IEEE Ind. Electron. Soc.*, Nov. 2010, pp. 3034–3039, doi: 10.1109/IECON.2010.5674947.

[52] K. Alluhaybi, X. Chen, and I. Batarseh, "A grid connected photovoltaic microinverter with integrated battery," in *Proc. 44th Annu. Conf. IEEE Ind. Electron. Soc.*, Oct. 2018, pp. 1597–1602, doi: 10.1109/IECON.2018.8591658.

[53] P. J. Chauhan, B. D. Reddy, and S. K. Panda, "Battery energy storage in standalone microgrid: Synchronization and transfer between operating modes," in *Proc. IEEE 7th Power India Int. Conf. (PIICON)*, Nov. 2016, pp. 1–6, doi: 10.1109/POWERI.2016.8077303.

[54] B. Amri and Soedibyo, "Design of batteries charging by charge management concepts on photovoltaic standalone system," in *Proc. Int. Seminar Appl. for Technol. Inf. Commun. (ISemantic)*, Aug. 2016, pp. 93–98, doi: 10.1109/ISEMANTIC.2016.7873816.

[55] *NREL's PV Watts Calculator.* Accessed. Feb. 12, 2020. [Online]. Available: https://pvwatts.nrel.gov.

[56] *State Load Dispatch Center.* Accessed. Feb. 12, 2020. [Online]. Available: https://www.delhisldc.org/Loadcurve.aspx

SIVASANKAR GANGATHARAN (Member, IEEE) received the B.E. degree in electrical & electronics engineering from Madurai Kamaraj University, Madurai, India, in 2002. He is the best outgoing student in the Department of Electrical and Electronics Engineering. He received the M.E. degree (Hons.) in power electronics and drives from Anna University, Chennai, India, in 2006, and the Ph.D. degree from Anna University. From 2006 to 2008, he was an Assistant Professor with VIT University. Since 2008, he has been with the Faculty of Electrical and Electronics Engineering, Thiagarajar College of Engineering, Madurai, where he is currently working as an Assistant Professor. He has published papers in international journals, and international and national conferences. His research interests include distributed generation, power quality, and power electronics and drives. He is also a member of the IEEE Society.

MAGESWARAN RENGASAMY received the B.E. degree in electrical & electronics engineering from Anna University, Coimbatore, India, and the M.E. degree in power system engineering from the Adhiyamaan College of Engineering, Hosur. He worked as an Assistant Professor with the Department of Electrical and Electronics Engineering, Akshaya College of Engineering and Technology, Coimbatore. He is currently working as a full-time Research Scholar with the Department Electrical and Electronics Engineering, Thiagarajar College of Engineering, Madurai. His research interests include renewable energy and smart grid, distributed generation, power system operation and control, power quality, intelligence control techniques, and demand side management.

RAJVIKRAM MADURAI ELAVARASAN received the B.E. degree in electrical & electronics engineering from Anna University, Chennai, India, and the M.E. degree in power system engineering from the Thiagarajar College of Engineering, Madurai. He worked as an Associate Technical Operations with the IBM Global Technology Services Division. He worked as an Assistant Professor with the Department of Electrical and Electronics Engineering, Sri Venkateswara College of Engineering, Chennai. He is currently working as a Design Engineer with the Electrical and Automotive Parts Manufacturing Unit, AA Industries, Chennai. He is also currently working as a Visiting scholar with the Clean and Resilient Energy Systems Laboratory, Texas A&M University, Galveston, USA. He has published papers in international journals, and international and national conferences. His research interests include solar PV cooling techniques, renewable energy and smart grids, wind energy research, power system operation and control, artificial intelligence, control techniques, and demand-side management. He received a Gold Medal for his master's degree. He is also a Recognized Reviewer in reputed journals namely IEEE SYSTEMS, IEEE ACCESS, *IEEE Communications Magazine, International Transactions on Electrical Energy Systems* (Wiley), *Energy Sources, Part A: Recovery, Utilization and Environmental Effects* (Taylor and Francis), *Scientific Reports* (Springer Nature), *Chemical Engineering Journal* (Elsevier), *CFD Letters*, and *3 Biotech* (Springer).

NAROTTAM DAS (Senior Member, IEEE) received the B.Sc. degree in electrical & electronics engineering from the Chittagong University of Engineering and Technology, Chittagong, Bangladesh, the M.Sc. degree in electrical & electronics engineering from the Bangladesh University of Engineering and Technology, Dhaka, Bangladesh, and the Ph.D. degree in electrical engineering from Yamagata University, Japan, in 2000. His Ph.D. research project was funded by the Ministry of Education, Science, Sports, and Culture of Japan (Japanese Government Scholarship). He has about 3-decades experience as an Academician and an Industrial Engineer in Australia and overseas. Before joining at CQUniversity as a Senior Lecturer of electrical engineering, he worked with USQ as a Lecturer of electrical engineering, a Research Fellow, a Lecturer, and an Associate Professor with Curtin University, Edith Cowan University, and Monash University, Australia. Earlier, he worked with NEC Yamagata Ltd., Japan, as a Senior Design Engineer. He is the author/coauthor of eight book chapters, over 160 peer-reviewed journals, and international conference papers. His research interests include power systems communication (smartgrids) using IEC 61850, multi-junction solar (PV) cells, modeling of high-efficiency solar cells (renewable energy), and high-speed communication devices (SOAs and MSM-PDs). He is also a Regular Reviewer of IEEE Transaction articles, IET articles, Elsevier, *Energies*, other similar journals, and conference papers. He has served as the Program Committee member for several IEEE conferences nationally and internationally as well as presented as an invited speaker. He is also a Senior Member of the IEEE PES and PHS, USA; a Fellow of the Institution of Engineers, Australia; a CPEng; and a Life Fellow of the Institution of Engineers, Bangladesh. He is also the Editor of the books *Nanostructured Solar Cells*, *Advances in Optical Communication*, *Optical Communication*, and *Optical Communication Systems*. He is also a Guest Editor of the Journal *Energies* Special Issue on Nanostructured Solar Cells.

EKLAS HOSSAIN (Senior Member, IEEE) received the B.S. degree in electrical & electronics engineering from the Khulna University of Engineering and Technology, Bangladesh, in 2006, the M.S. degree in mechatronics and robotics engineering from International Islamic University Malaysia, Malaysia, in 2010, and the Ph.D. degree from the College of Engineering and Applied Science, University of Wisconsin–Milwaukee (UWM). He has been working in the areas of distributed power systems and renewable energy integration for the last ten years, and he has published several research articles and posters in this field. He is currently involved in several research projects on renewable energy and grid-tied microgrid system with Oregon Tech, as an Associate Professor with the Department of Electrical Engineering and Renewable Energy. He is also a Senior Member of the Association of Energy Engineers (AEE). He is also working as an Associate Researcher with the Oregon Renewable Energy Center (OREC), Oregon Institute of Technology. He is also a registered Professional Engineer (PE) in the state of Oregon, USA. He is also a Certified Energy Manager (CEM) and a Renewable Energy Professional (REP). His research interests include modeling, analysis, design, and control of power electronic devices, energy storage systems, renewable energy sources, the integration of distributed generation systems, microgrid and smart grid applications, robotics, and advanced control systems. He was the winner of the Rising Faculty Scholar Award from the Oregon Institute of Technology, in 2019, for his outstanding contribution in teaching. He, with his dedicated research team, is looking forward to exploring methods to make electric power systems more sustainable, cost-effective, and secure, through extensive research and analysis on energy storage, microgrid systems, and renewable energy sources. He is also serving as an Associate Editor for IEEE Access.

VARATHARAJAN MEENAKSHI SUNDARAM graduated the B.E. degree in electrical & electronics engineering from Anna University, Chennai, India, in 2007. He received the M.E. degree in control & instrumentation from Anna University, in 2012. Since 2012, he has been working as an Assistant Professor of electrical and electronics engineering with the Thiagarajar College of Engineering, Madurai, India. His research interest includes state estimation, control & optimization.

• • •